Deep–Sea Research I 182 (2022) 103704

Contents lists available at ScienceDirect

Deep-Sea Research Part I

journal homepage: www.elsevier.com/locate/dsri

Community composition and spatial energetics of mesopelagic fishes and squids in the eastern Bering Sea as influenced by habitat variables

E.H. Sinclair [a,*], N.A. Pelland [b,c], D.S. Johnson [d]

[a] Wish Creek Research, LLC, P.O. Box 906, Twisp, WA, 98856, USA
[b] Cooperative Institute for Climate, Ocean, and Ecosystem Studies, University of Washington, 3737 Brooklyn Ave N.E., Seattle, WA, 98195, USA
[c] National Marine Mammal Laboratory, Alaska Fisheries Science Center, Building 4, 7600 Sand Point Way N.E., Seattle, WA, 98115, USA
[d] Protected Species Division, Pacific Islands Fisheries Science Center, 1845 Wasp Boulevard, Building 176, Honolulu, HI, 96818, USA

ARTICLE INFO

Keywords:
Bering sea
Mesopelagic
Micronekton
Energetics
Mesoscale physics
Community ecology
GLMs

ABSTRACT

Micronekton of the mesopelagic zone (200 m–1000 m depth) play a central role in most aspects of global marine ecology linking epipelagic and deep scattering layers as planktivores, carnivores and principal prey to both shallow diving and deep living apex predators. Yet, despite this critical role and conspicuous presence, little is known regarding most aspects of mesopelagic community ecology, including habitat associations at sub-basin spatial scales. Here we address several aspects of these data deficiencies in the eastern Bering Sea mesopelagic – a highly productive subarctic marine ecosystem home to multiple protected predator species and large commercial fisheries. Through 41 midwater trawls conducted at 250 m, 500 m and 1000 m depths during May of 1999 and 2000, and a series of generalized linear models and cluster analyses, we describe the influence of remotely sensed oceanographic habitat variables on the diel distribution, relative abundance and community composition of 30 species of mesopelagic fish and squid in 3 contrasting study areas. We then project the total energy available to predators at depth and across the eastern Bering Sea Basin based on the identified habitat constraints. Fishes from the families Bathylagidae and Myctophidae, and squids from the Gonatidae dominated the 72 species catch biomass (n = 225,000, 2,100 kg). The six most abundant species were equally divided between each of the three dominant families and are also the most highly represented mesopelagic species in eastern Bering Sea pelagic predator diets. Their association with surface habitat variables describe a complex and multifaceted relationship between physical/biological predictors and the total mesopelagic energy field during the spring bloom period in this ecosystem. *Leuroglossus schmidti*, *Bathylagus pacificus*, *Stenobrachius leucopsaurus*, *S. nannochir*, *Gonatopsis borealis* and *Eogonatus tinro* contrast in the suite of physical and biological variables that they respond to, and also in the character of their response. Although L. *schmidti* is of moderate caloric value, it expressed the greatest overall energy signature at all depths due to its overwhelming biomass, and response to the presence of specific, variable habitat conditions across extensive portions of the study area. Interannual variability in habitat variables forecasted a pronounced redistribution of dominant species and thereby total mesopelagic energy content – providing a potential mechanism for shifts in central-place predator habitat use, energy expenditure, and diet. The known relevance of mesopelagic species as prey and the energetic potential for apex predators foraging in the Basin illustrates a cautionary narrative regarding unregulated harvest of biota from this poorly understood and critically important oceanic zone.

1. Introduction

Fishes and squids of the mesopelagic zone (200–1000 m) play a key trophic role as both predator and prey and their biomass is estimated to exceed that of currently commercially exploited species by orders of magnitude (Irigoien et al., 2014). They are predaceous on copepods, euphausiids and other micronekton including other fishes and squids, and are pervasive in the diets of a broad spectrum of upper pelagic predators (Beamish et al., 1999). The fish families Myctophidae and Bathylagidae and squid family Gonatidae dominate the pelagic diets of commercial fishes (pollock, salmon, black cod) and squids (Sinclair, 1991; Beamish et al., 1999), marine mammals (Crawford 1981; Walker

* Corresponding author.
E-mail address: beth.sinclair@noaa.gov (E.H. Sinclair).

https://doi.org/10.1016/j.dsr.2022.103704
Received 17 April 2021; Received in revised form 13 January 2022; Accepted 25 January 2022
Available online 31 January 2022

and Jones, 1991; Beamish et al., 1999; Sinclair et al., 1999) and birds (Sinclair et al., 1999, 2008) in the North Pacific Ocean and Bering Sea. In addition, mesopelagic micronekton play a significant role in the ocean's biological carbon "pump" – the downward flux of organic carbon from the ventilated ocean surface (Falkowski et al., 2000; Hidaka et al., 2001; Parekh et al., 2006; Radchenko, 2007; Anderson et al., 2019) – through respiration and excretion of organic matter at depth, direct transport of carbon during daily vertical migration, and consumption by larger nekton migrating upwards from the benthic (Willis and Pearcy, 1982; Longhurst and Harrison, 1988; Jónasdóttira et al., 2015).

Despite their importance to the oceanic ecology and climate system, and their potential for exploitation by commercial fisheries, micronekton of the mesopelagic zone are understudied in comparison to other marine resources (St. John et al., 2016). In particular, links between oceanographic variables and mesopelagic biomass, including 'species traits and habitats' are poorly understood. A greater understanding of these links would improve prediction of species dynamics relative to oceanographic regimes, and help to predict how those dynamics will likely be impacted as the environment alters under climate change (St. John et al., 2016). There is also an urgent need to further define the role of the mesopelagic community in the food web in various marine ecosystems, particularly the dependence of predators on mesopelagic prey, including those managed as protected species within a national or international regulatory framework.

These needs are acute in the eastern Bering Sea (EBS), where mesopelagic fishes and squids are significant components in the diet of multiple marine species including the northern fur seal (*Callorhinus ursinus*) currently listed as depleted under the Marine Mammal Protection Act (NOAA National Marine Fisheries Service, 2007). The Bering Sea Basin and continental slope, adjacent to the subarctic North Pacific Ocean and arctic Chukchi Sea, are highly productive oceanographic regions critical to protected marine mammals and fishes of commercial importance (Beamish et al., 1999; Benoit-Bird et al., 2013a, b; Paredes et al., 2012, 2014) but infrequently studied in the context of mesopelagic fishes and squids (Sinclair et al., 1999). The Bering Sea Basin has rich potential for study of mesopelagic micronekton as highlighted by previous research describing the biological importance of the basin to predator species (*see*: Antonelis et al., 1997; Loughlin et al., 1999; Sinclair et al., 2008) the significance of mesopelagics in the diet of these predators, and fine-scale behavioral associations of predators with oceanographic variability (Hunt et al., 2002). Although broadly viewed as significant, direct linkages between the mesopelagic prey field, its species composition, and the environment, through *in situ* observation, have been more rare in this ecosystem. In a survey of mesopelagic fishes that included the EBS, Pearcy et al. (1979) found evidence for basin-scale shifts in species composition and hypothesized that these were related to variations in water masses found along the southeastern continental slope. However, their observations were not sufficiently dense to investigate finer-scale variability. Further *in situ* observations are needed in order to understand mesopelagic community composition and habitat associations, and their potential implications for top predator foraging, in this region.

The southeastern Bering Sea Basin offshore of the continental shelf (Fig. 1a) features a unique eastern boundary current system whose characteristics contribute to the high rates of ecosystem productivity. The mean currents include the poleward flowing Aleutian North Slope Current (ANSC) (Reed and Stabeno, 1994, 1999; Stabeno et al., 2009) and Bering Slope Current (BSC) (Johnson et al., 2004; Ladd, 2014), which transport water that has entered the basin from the Aleutian passes along the continental shelf edge and slope (Fig. 1a). The BSC is a

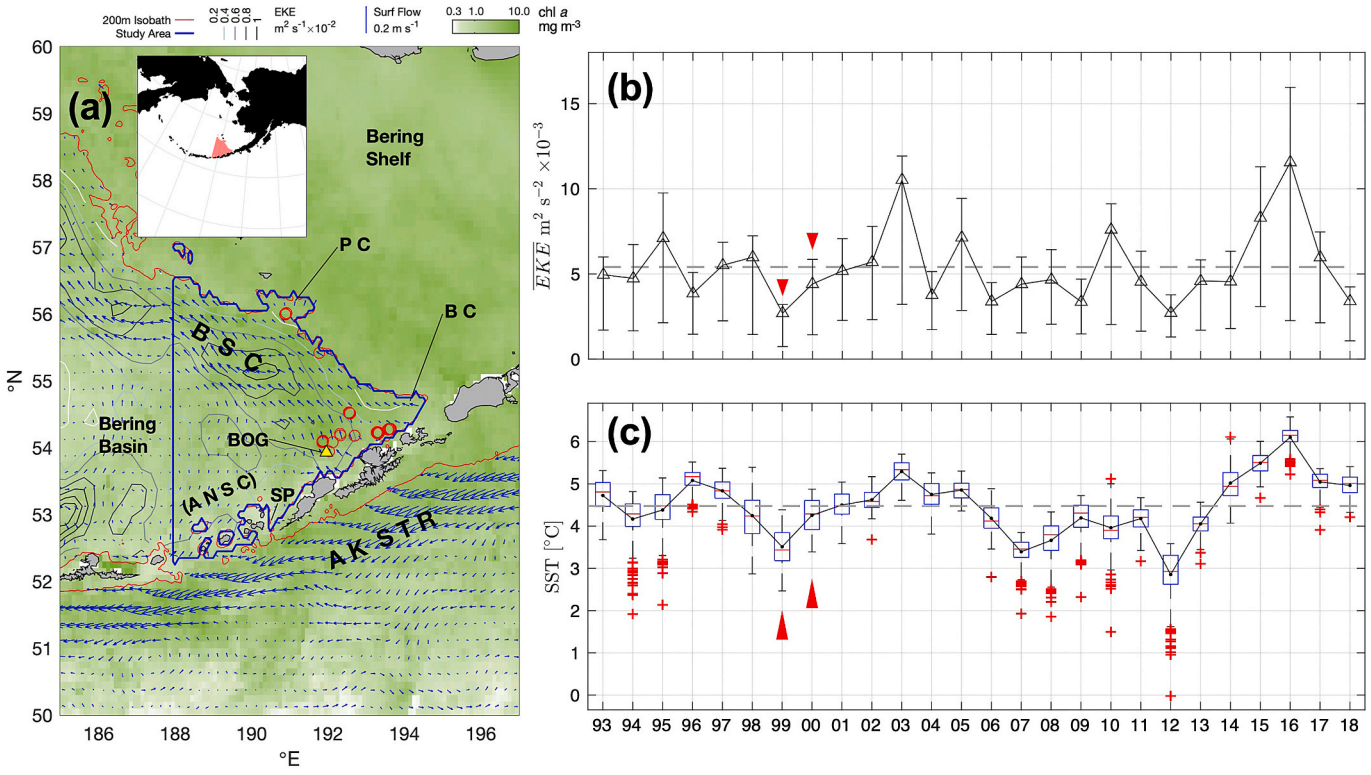

Fig. 1. (a) Large- and small-scale location overview of 41 day and nighttime trawls off-shelf at 250 m, 500 m and 1000 m. Haul locations within southeastern Bering Sea Basin and surroundings, overlaid on climatological May chlorophyll (background color), surface flow (blue arrows), and eddy kinetic energy (EKE, gray contours, scales for all variables at top). Red contours indicate the 200 m isobath (shelf break edge), red circles indicate haul locations, and dark blue outlines the expanded study area. Labels indicate prominent oceanographic or topographic features. BSC: Bering Slope Current, ANSC: Aleutian North Slope Current, AK STR: Alaska Stream, PC: Pribilof Canyon, BC: Bering Canyon, BOG: Bogoslof Island, SP: Samalga Pass. Panels show interannual variability in (b) mean and interquartile range of eddy kinetic energy; and (c) sea surface temperature (SST) box plots in the southeast Bering Sea in May. Study years are indicated in panels b and c by triangles.

meandering eastern boundary current with robust variability including both enduring and transitory eddies that demonstrate a high degree of interannual variability, possibly forced by wind stress patterns across the subarctic North Pacific region (Stabeno et al., 2009; Ladd et al., 2012; Panteleev et al., 2012; Ladd, 2014; Prants et al., 2019) (Fig. 1b). Interactions between eddies, topography (e.g. canyons) and currents in this region provide a mechanism for on/off-shelf exchange in addition to upwelling of nutrient-rich water (Stabeno and Van Meur, 1999; Mizobata et al., 2006; Ladd 2014; Stabeno et al., 2016). Such mesoscale activity is a major contributor to the Bering Sea 'Green Belt' (Springer et al., 1996; Ladd et al., 2012) where bottom-up forcing provides increased primary productivity, biomass, and abundance of zooplankton and secondary trophic level organisms on which many mesopelagic species feed and to which upper trophic levels congregate. There is evidence that predator species in the Bering Sea Basin – including northern fur seals (Sterling 2009; Nordstrom et al., 2013), black-legged kittiwakes (Paredes et al., 2014), and murres (Kinder et al., 1983; Schneider et al., 1990) – alter their foraging behavior in response to physical variability associated with the BSC. Both northern fur seals and black-legged kittiwakes are significant predators of mesopelagic fishes and squids and especially of *Leuroglossus schmidti* (Sinclair et al., 2008). This is broadly consistent with evidence from other ecosystems, in which physical mesoscale variability has been shown to alter, enhance, or concentrate mesopelagic prey assemblages, potentially due to local trapping, alterations in thermal structure, or over longer time scales, enhancement in local productivity (Godø et al., 2012; McGillicudy, 2016; Della Penna and Gaube, 2020). Direct evidence of these effects in the Bering Sea is more sparse, and refining our understanding of how the mesopelagic prey field responds to eddying flow, in addition to other dynamic habitat covariates, can provide a framework for approaching interannual variability in this region.

Here, we present a multidisciplinary analysis of previously collected observations of the mesopelagic prey field in the southeast Bering Sea Basin (Sinclair and Stabeno, 2002), and evaluate its relationship to features of the physical environment influencing distribution and abundance of species and their associated communities and subsequent

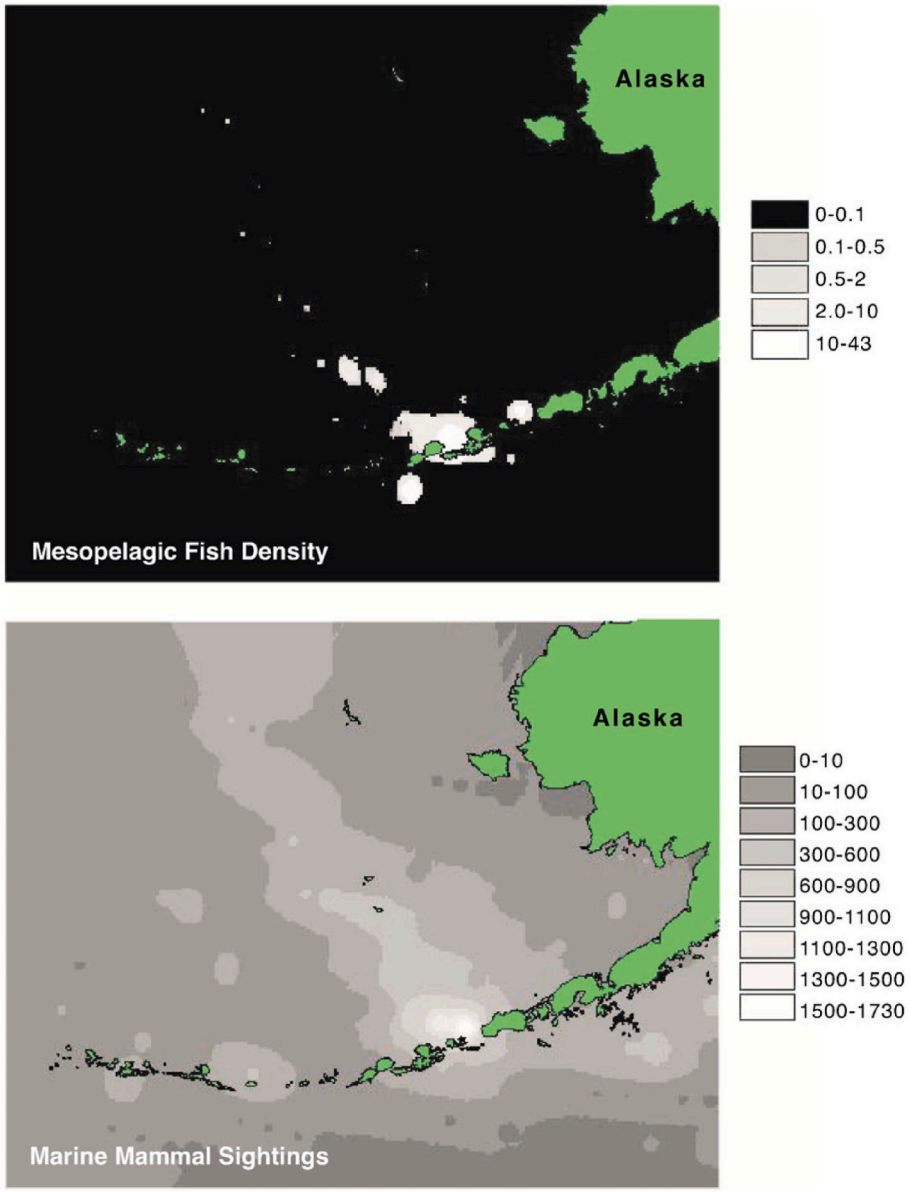

Fig. 2. Mesopelagic fishes density (kg/ha) as determined from bycatch estimates in research bottom trawls conducted across the continental shelf to slope edge in the eastern Bering Sea, 1978–1991; and opportunistic marine mammal sightings 1958–1997 within and outside the green belt area of the eastern Bering Sea. (Figure reprinted with permission, Sinclair and Stabeno, 2002).

energetic potential to predators at depth. In this work our goals were to identify: 1) species and community composition, distributions and relative diel abundances at depth in the observations; 2) statistical relationships between dynamic physical and biological habitat variables and species distributions, and comparison of responses across species; and, 3) the implications of these relationships for variations in total energy in the mesopelagic prey field, dielly at depth and across the EBS Basin.

Specifically, we evaluate the relationship between biological (surface chlorophyll) and physical oceanographic variables, mesopelagic community composition and species-specific distributions at each of our three study sites associated with the Bering Sea Greenbelt (Fig. 2). The oceanographic predictor variables we use are derived from widely-available remotely-sensed indicators of the ocean surface. While surface variables are not direct observations of habitat at depths that mesopelagic species mostly inhabit – and may have diminished ability to predict assemblage with increasing depth (Vecchione et al., 2015) – they have nonetheless been shown in other instances to relate to mesopelagic variations at a variety of scales (Proud et al., 2017; Della Penna and Gaube, 2020). Remotely-sensed variables are also more consistently available than *in situ* observations at depth in the EBS Basin (Capotondi et al., 2019). We elect to make this tradeoff in order to facilitate the prediction of mesopelagic species distributions outside our sample areas, yet within the established EBS ecosystem, and for the same month in other years. Species-specific energetic values are then applied to these distributions to project the energetic potential available to predators at various depths across the Bering Sea Basin. Finally, we discuss the implications of these maps of variations in the location of mesopelagic nekton and how these results can guide directions of future observational study.

2. Methods

2.1. The study area and biological sampling protocol

This study is based on collections made in May 15–20, 1999 and May 15–22, 2000 within the Bering Sea Greenbelt in Bering and Pribilof Canyons, and near Bogoslof Island (53° 55′ N 168° 02′ W) – sites of contrasting physical settings and oceanography in the EBS (Fig. 1a). Sample collection dates were selected to capture the season of the strongest annual pulse of primary and secondary production, and the migration and foraging concentrations of mesopelagic predators from the northern North Pacific into the EBS (Hunt et al., 2002). The general sample station locations were selected based on the highest density of bycatch records of mesopelagic fish families Bathylagidae and Myctophidae in National Marine Fisheries Service (NMFS) commercial species groundfish research trawls (1978–1991) and Platforms of Opportunity (POP) opportunistic marine mammal sightings (1958–1997) data records (Sinclair et al., 1999) (Fig. 2). Sea surface temperatures (Fig. 1c) were below-average in May 1999 and close to average in May 2000 in the southeast Bering Sea Basin. Temperatures in the upper permanent pycnocline (100 m depth; not shown) were relatively typical of NOAA Pacific Marine Environmental Laboratory surveys 1994–2015, with the 1999 survey somewhat cooler at depth than 2000.

Our catch analyses are based on a haul-by-haul evaluation of the diel distribution, numbers, weight, individual body size and caloric value of fish and squid species collected day and night at 250 m, 500 m and 1000 m at 41 sampling stations. Fishing was conducted aboard the now retired NOAA research vessel *Miller Freeman* with an open mouth (avg vertical and horizontal opening during fishing 25 m × 40 m) pelagic Aleutian Wing rope trawl fitted with a knotless, 1.2 cm stretch mesh lining the cod end designed by the NOAA Alaska Fisheries Research Center net loft, specifically for this mesopelagic fishing effort. The trawl was towed on a double warp (headrope and footrope measurements of 81.7 m, and mesh size tapering from 8.9 to 3.3 cm). The net design, oblique net drop, haul-back and ship speed (3.5 kts at fishing depth) were conducted in a manner that emphasized catch from specific depths within the mesopelagic zone following a midwater open mouth trawl technique pioneered by Russian researchers that included increased trawl speed at deployment and decreased speed at retrieval in order to reduce bycatch from depths shallower than target depth (Balanov and Il'inskii, 1992; *see*: Sinclair et al., 1999; Sinclair and Stabeno, 2002). Increasing trawl speed at deployment also kept the doors from flipping and the net from collapsing. A minimum of one daytime and one nighttime trawl was conducted at each of the three depths at each of the three general sampling stations in order to capture the effects of diel vertical migration on patterns of distribution and abundance.

With the exception of time gaps in fishing effort due to net drop, haulback, sort time, net repair or replacement, trawls ran continuously over a 24-h period at each sampling station standardized to 30 min tows at fishing depth. Operations were suspended if the net was judged to be fishing irregularly based on wheelhouse observations of real-time net behavior or conditions creating excessive variability from standard protocol. The ship drifted during gaps in fishing effort then returned to the sampling end-point so that day and nighttime trawls were conducted at each new depth over the same location with a minimum of 2 h 'rest' time in the water column. Real time fishing, fishing bottom depth and mouth opening were recorded with a bathythermograph (MBT) attached to the net. To ensure fishing location was above bottom and within the basin, bottom depth at sample station and along the expanded sampling region (Fig. 1) was verified retroactively from the NOAA ETOPO1 1 arc-minute dataset (Amante and Eakins, 2009).

Taxonomic separation of mesopelagic micronekton is especially challenging due to the structural damage incurred when samples are harvested from 1000 m ocean depths. For that reason, the entire sample of squids and most species of fish were flash frozen and transported back to the laboratory for detailed identification confirmation and examination. Exceptions to whole haul sampling were for fishes *Leuroglossus schmidti* and mixed species of the genera *Stenobrachius* and *Bathylagus* which were caught in volumes too large for reasonable transport. These were separated from other species in the field, weighed en masse, then 20% of the total weight was randomly sub-sampled and frozen for return to the laboratory. Species identifications were confirmed in the laboratory based on specific structural features including sucker and hook patterns in squids and photophore placement and count in fishes. For individuals in quality condition, length (cm) and weight (g) were measured and hard and soft tissues were extracted for body size regression analysis and energetic composition respectively (*see*: Sinclair et al., 2015, 2016). Field and laboratory numbers and weights were combined retroactively for final computation of biomass at each haul site by depth and time of day. The numbers and weights of mixed species of *Stenobrachius* and *Bathylagus* that were sub-sampled in the field were re-combined proportionally after determination of relative proportion in the laboratory.

2.2. Model descriptions – species occurrence, biomass, community composition and energetics

2.2.1. General approach

Thirty species for which we had energetic profiles were selected to model the influence of depth, time of day, and habitat covariates on species occurrence and relative biomass between hauls. These covariates were then used to predict species occurrence, distribution, and biomass over an expanded study area into the greater Bering Basin. Based on these models, a 3-dimensional map of the energetic potential presented by species and community guilds across the expanded study area is projected.

2.2.2. Tweedie GLMs

We fitted Generalized Linear Models (GLM) to total catch weight data for each species in our hauls. The GLM for each species included terms due to depth of haul (250 m, 500 m, 1000 m), time of day (day/

night), and habitat covariates. A total of seven habitat covariates were used: Chlorophyll *a*, Sea Surface Temperature (SST), SST anomaly from a zonal mean (SSTa), sea level anomalies (SLA), finite size Lyapunov exponents (FSLE) – as a measure of frontal activity, distance to front (DTF), and geostrophic current speed (GCS). Rather than multi-model fitting and selection for each species, we used a regularization constraint on the GLM coefficients, described below. This constraint, which imposes penalties for inducing sparseness in the GLM coefficients, allows us to simultaneously estimate coefficients and select covariates that are important to prediction.

To model total catch weight, we used a Tweedie distribution (Shono, 2008) to account for extra zeroes due to species absence in a specific trawl and variance over-inflation due to clustering of size classes. If y_{ij} for a recorded response of species $i = 1, \ldots, I$ in the j th haul ($j = 1, \ldots, J$), then we model the response as

$$y_{ij} \sim \mathrm{TW}_{p_i}\left(y_{ij} \middle| \mu_{ij}, \varphi_i\right),$$

where, $\mathrm{TW}_p(\cdot|\mu, \varphi)$ refers to a Tweedie distribution (*see*: Dunn and Smyth, 2005) with mean μ and variance parameter φ, for index $1 < p < 2$. For this analysis, the mean function was modeled with the log link.

$$\log(\mu_i) = X\beta_i,$$

where X is a design matrix with habitat and haul specific covariates.

The Tweedie distribution is especially appropriate for modeling total catch weight as it can possess both zero-inflation and over-dispersion within the same model. Both of these data issues may be present as species may be completely absent from a haul (i.e., structural zero) and over-dispersed because of clustering of individuals. For a $\mathrm{TW}_p(\mu, \varphi)$ model the mean, variance, and zero-inflation are given by the functions

$$\begin{aligned} E(Y) &= \mu \\ Var(Y) &= \varphi\mu^p \\ P\left(Y = 0\right) &= 1 - \exp\left\{ -\frac{\mu^{2-p}}{\varphi(2-p)} \right\}. \end{aligned}$$

Habitat covariates were selected based on variables previously associated with the distributions of mesopelagic fish and squid species or their foraging predators (*see* Introduction). For chlorophyll-*a*, $\log_{10}$ transformed monthly composite 9 km spatial resolution SeaWiFS surface concentrations (NASA OBPG, 2018) were used as a proxy for phytoplankton biomass. Remotely-sensed (SSTs) were obtained from the daily NOAA OISST V2 High-Resolution dataset (Reynolds et al., 2007). Remote SSTs interpolated to haul locations and times were positively correlated with temperature at 100 m depth during both surveys ($r^2 = 0.63$, $p < 0.0001$, root-mean-square difference: 0.35 °C). The SST anomaly (SSTa) from a zonal average 170°E - 210°E at each latitude was estimated to highlight onshore-offshore temperature contrasts between ANSC/BSC surface waters and the interior basin (Fig. SI 1).

Sea level anomalies (SLA; deviations from a time-average, representative of eddies and meanders), were obtained from the delayed-time all-satellite merged SSALTO/DUACS L4 SLA product. The daily spatial average between 52°N-57.5°N, 188°E-196°E was subtracted to remove signals due to uniform surface heating (Chelton et al., 2011; Ladd, 2014). These SLAs were positively correlated with survey temperature ($r^2 = 0.75$, $p < 0.0001$) and negatively correlated with survey salinity ($r^2 = 0.38$, $p < 0.0001$) at 100 m depth. Finite size Lyapunov exponents (FSLEs; d'Ovidio et al., 2004) which identify transport barriers or vortex boundaries and are commonly used as proxies of frontal regions (*cf.* Nordstrom et al., 2013), were obtained from the AVISO + experimental FSLE dataset. Distance to front (DTF) was defined based on fronts with FSLE magnitude ≥ 0.2 d^{-1}, consistent with Nordstrom et al. (2013). Geostrophic current speeds were derived from the SSALTO/DUACS L4 Absolute Dynamic Topography (ADT) product, which includes both time varying and mean flows. High-pass spatial filtered ADT was used to estimate eddy kinetic energy (*cf.* Panteleev et al., 2012) values shown in Fig. 1.

For chlorophyll, gaps in the monthly composite images due to persistent cloud cover in the Bering Sea were filled using local Gaussian Markov Random Field (GMRF) spatial models. Each gap in the image raster was buffered by observed cells, then a GMRF model was fit with the rook neighborhood structure to the missing cells and their buffer cells. The value of the missing cells was then predicted with the fitted spatial model. For all covariates, a 60 km buffer radius was used, with the exception of Chlorophyll-*a* for which a spatial model was fitted to the entire image, not just local missing sections because the patches were too numerous and small for the local approach to provide computational advantage.

To facilitate prediction outside the haul locations, prior to model fitting habitat covariates were converted from continuous to categorical ("low," "neutral," "high" categories), such that an equal number of samples fall into each category – i.e., the boundaries between categories are chosen at the 1/3 and 2/3 level of the empirical cumulative distribution. This approach necessarily reduces the resolution of the covariates used to fit the data, with the tradeoff that any predictions outside the sampled values are more stable because extrapolation is effectively avoided. The values of the remotely-sensed covariates interpolated to the hauls are within the center of the distribution of values in the SE Bering Basin in May over available years (Fig. SI 2). The time of the haul was categorized as "day" or "night" depending on the solar elevation at the location and date of the haul. Hauls with negative solar elevation were categorized at "night" or "day" for positive solar elevations.

2.2.3. Sparse GLMs for predicting total catch mass

Because there are only $J = 41$ samples (hauls) and $K = 9$ possible effects for each species (depth, day/night, and 7 habitat covariates) there is not a large amount of information for which to make precise estimates of each β_{ik}, therefore, we place a regularization constraint (*sensu* Wood, 2017) on the parameters. For covariates that have little effect on the observed total catch weight, estimates of their associated coefficients will go to zero more precisely. In this way, this constraint takes the form of a normal density prior distribution for each β_{ik}. Thus the log likelihood which is maximized is

$$L(\boldsymbol{\beta}_i, \varphi_i, p_i) = \sum_{j=1}^{J} \log \mathrm{TW}_{p_i}\left(y_{ij} \middle| \exp\left(\mathbf{x}_{ij}'\boldsymbol{\beta}_i\right), \varphi_i\right) - \sum_{k=1}^{K} \frac{1}{2}\lambda_{ik}\boldsymbol{\beta}_{ik}'\boldsymbol{\beta}_{ik},$$

where $k = 1, \ldots, K$ indexes an "effect" in the model and $\boldsymbol{\beta}_i = (\boldsymbol{\beta}_{i1}, \ldots, \boldsymbol{\beta}_{iK})$. The penalty parameter λ_{ik} determines the strength of the penalty and the amount of regularization for $\boldsymbol{\beta}_{ik}$. Essentially, large λ values imply that a covariate is not significantly contributing to the model fit, thus selecting it out as part of the likelihood maximization. As λ_{ik} becomes large $\boldsymbol{\beta}_{ik} \to 0$. Note that for each effect there are several coefficients. This is because categorical covariates with multiple levels are all penalized simultaneously by a single λ_{ik}. For example, the influence of a covariate is governed by three coefficients, one for each level of the discretized habitat, that is $\boldsymbol{\beta}_{ik} = (\beta_{ik,low}, \beta_{ik,med}, \beta_{ik,high})'$ for the k th habitat variable. As $\lambda_{ik} \to \infty$, all three tend to 0 simultaneously, eliminating that effect from the model.

For fitting these sparse GLMs, we used the R statistical environment (R Core Team, 2019) with package mgvc (Wood, 2011) to estimate the model parameters using Restricted Maximum Likelihood (REML). Wood et al. (2016) provide methodology for making statistical inference for these models accounting for estimation of the penalty terms which is available in the mgcv package. Thus, the optimization of the model itself eliminates covariates that are not contributing "significantly" to the model fit, as well as, inflating standard errors to account for the added regularization procedure.

2.2.4. Predicting relative energy content

Once the $\mathrm{TW}_p(\cdot|\mu, \varphi)$ model has been fitted to each species, we

predicted what total catch might be observed for each species in a different location and/or year (i.e. different habitat conditions). The remotely-sensed data were used to calculate habitat covariates at unsampled locations in the basin in May, both within and outside the study years. Remotely-sensed data were interpolated to a 0.1° resolution spatial grid and the same categorical boundaries as used in model fitting were used to convert gridded variables to categorical values. The data were compiled within an expanded study area (Fig. 1a) representing a nearby region where covariate relationships to species occurrence might reasonably be expected to hold based on consistency in water mass properties, temperatures, dynamic oceanographic processes, productivity, and trophic relationships (Springer et al., 1996; Antonelis et al., 1997; Loughlin et al., 1999; Sinclair et al., 1999; Sinclair et al., 2008; Belkin, 2016, Fig. 1a). Model predictions are evaluated only for points inside the Bering Sea, between 52°N-57.5°N latitude and 188°E-196°E longitude, and with bottom depth exceeding 200 m. The boundaries and spatial extent of the expanded study area into the greater EBS Basin were established conservatively based on the individual restrictions and best representation of the remotely sensed variables within and outside our specific study years (Fig. SI 3).

For each different year and location, indexed by j^*, the predicted catch for species i, was estimated as $\widehat{y}_{ij^*} = \exp(\boldsymbol{x}_{ij^*}{}'\widehat{\boldsymbol{\beta}}_i)$. The total energy index for that year and location is the weighted sum over all species, that is,

$$\widehat{E}_{j^*} = \sum_i W_i \widehat{y}_{ij^*},$$

where W_i is the average per kg caloric content of individuals of the ith species. Mean energy values for mean body size, total number and total catch weight by haul were used in the final models.

2.2.5. Predicting community composition

In addition to predicting species total energy and mass separately, we investigate whether prediction gains could be made by collapsing individual responses into species guild responses. Species guild responses are shared among all species that belong to a particular guild, that is $\boldsymbol{\beta}_i = \boldsymbol{\beta}_g$ for all species i that belong to guild g. Johnson and Sinclair (2017) investigated a model that simultaneously estimated guild membership and response, but it was too computationally intensive for regular use. Therefore, in order to investigate similarities in species response to the environmental conditions, as well as similarities in vertical migration patterns, we performed a K-means clustering analysis (MacQueen, 1967) on the regression coefficients obtained in the penalized GLM fitting on the 14 most prominent species captured in the trawls. This was done more as a way to describe the results of the individual fits, rather than full inference for the guild membership. All haul depths were represented in the selection of these 14 species, each of which were known to predominate in Bering Sea pelagic predator diets and numbered at least 75 individuals in each of the two study years. The sample size cutoff was based on field observations of species patterns with haul depth and considered the minimum required to reflect definitive species distribution rather than bycatch between depths based on these observations. The selected species were primarily from the three families (Myctophidae, Bathylagidae and Gonatidae) that dominate abundance and biomass both in our hauls and in Bering Sea predator diets (Beamish et al., 1999; Sinclair et al., 2008).

The K-means analysis is intended to be a descriptive analysis aimed at describing similarities among species response and not necessarily a fully model-based clustering as presented in Johnson and Sinclair (2017). To perform this analysis the coefficients from the GLM fitting were extracted for each species and split into those associated with environmental response and those associated with vertical migration patterns. Then the coefficients were treated as observations from each species and clustered by K-means. We chose the number of groups to be the smallest number such that at least 90% of the total variation in the coefficient values was retained by using cluster centers for each species, that is variation between cluster centers was at least 90% of the variation in the original coefficient estimates.

3. Results

3.1. Hauls, interannual catch and community composition

Forty-one hauls were conducted in 1999 (n = 14) and 2000 (n = 27) in three contrasting study areas including near Bogoslof Island (1999, n = 5; 2000 n = 9), in and near Bering Canyon east slope (1999 n = 8; 2000 n = 11) and in and southeast of Pribilof Canyon (1999 n = 1; 2000 n = 7) (Fig. 1a). In 1999, a total of 8 daytime (250 m = 2, 500 m = 3, 1000 m = 3) and 6 nighttime hauls (250 m = 3, 500 m = 1, 1000 m = 2) were conducted. In 2000, a total of 16 daytime hauls (250 m = 6, 500 m = 5, 1000 m = 5) and 11 nighttime hauls (250 m = 6, 500 m = 4, 1000 m = 1) were conducted.

3.1.1. Total catch values

All hauls together yielded 72 species of fish (n = 55) and cephalopods (n = 14 squids; n = 3 octopods) (Table 1). Despite marked differences in catch volume between years for some of the predominant species, the total catch number and mass of all samples combined was similar between years and together yielded approximately 225,000 individuals with a biomass of 2,100 kg (Table 1). Non-target species caught incidentally were recorded then excluded from further analyses including summary values for catch mass. These generally consisted of species that spend some portion of their lives at mesopelagic depths, but are not considered exclusive to the mesopelagic; are not 'micronektonic' as adults; or, do not fall under the taxonomic categories of fishes and cephalopods. 'Incidental' species included: walleye pollock (*Gadus chalcogramma*), sablefish (*Anoplopoma fimbria*), grenediers (*Albatrossia pectoralis*, *Coryhaenoides acrolepis, C. cinereus*), Pacific sleeper shark (*Somniosus pacificus*), unidentified deep sea shrimps, Scyphozoa, salps, unidentified jellyfish, and unidentified sea cucumber (*Holothuroidea*).

The highest catches overall were driven by members of two families of fishes – the deepsea smelts, Bathylagidae, and lanternfishes, Myctophidae – and a single family of cephalopod squids, Gonatidae (Table 1). *Leuroglossus schmidti* was present in every haul and dominated the bathylagid catch by number and biomass as well as the overall total catch (67% of total catch number, 54% of total catch wt). The second highest species catch in terms of number was the myctophid *Stenobrachius leucopsarus* (16% of total catch number, 8% of total catch wt) which, like *L. schmidti* was present in every haul. The bathylagid *Bathylagus pacificus* was the third ranked species in terms of number of individuals caught (7% of total catch number), but due to an average individual weight 3 times that of *S. leucopsarus* it ranked second highest in terms of the percent of total catch weight (17% of total catch wt). The fourth most highly ranked species in terms of number caught in both years combined (n = 12,244; 90 kg) was the myctophid *S. nannochir*. Although the total number of individuals caught ranked this species as fourth in numerical dominance, the biomass of *S. nannochir* was less than that of *Gonatopsis borealis* (93 kg) a gonatid squid represented by just 1,930 individuals (Table 1). Bathylagid and myctophid fishes outranked the abundance and mass of squids overall; however, among the Gonatidae, *G. borealis*, *Eogonatus tinro* and *Berryteuthis magister* were the next most highly ranked species caught, in that order (Table 1).

Leuroglossus schmidti dominated the catch in both years of the study. However, the catch number of this species was reduced by over 35% in 2000 and biomass was 16% less than 1999 values (Table 1). This reduction in catch occurred despite the fact that *L. schmidti* is present in all hauls, the hauls were similarly spread between depth and time of day between years, and the number of hauls conducted in 2000 doubled. All four species of bathylagids decreased in total number and biomass between 1999 and 2000 (Table 1). In contrast, all but one *(Nannobrachium regale)* of the 7 species of Myctophidae increased in the second year of

Table 1
The total number, mass and body size of the 77 species caught in eastern Bering Sea mesopelagic surveys conducted in 1999 and 2000. The 30 species selected for modeling the community composition, distribution and projected energy contribution beyond the mesopelagic survey study area into unsampled regions of the eastern Bering Sea basin are noted ([a]). Mean energy values for mean body size and total catch weight by haul were used in the final models.

Species	1999 Number	Mass (g)	Standard Length Range (mm)	2000 Number	Mass (g)	Standard Length Range (mm)	Energy (cal/100 g)
Albatrossia pectoralis	41	11156	39–230	72	18425	48–188	121
Alepisaurus ferox	1	4918	1140	0	0	NA	
Aptocyclus ventricosus	2	<1000	92–265	0	0	NA	
Arctozenus risso	0	0	NA	1	25	247	
Avocettina gilli	11	110	400–525	0	0	NA	
Avocettina infans	0	0	NA	18	NA	68–505	
(Psuedobathylagus) milleri[a]	139	5721	69–190	64	1228	77–178	108
Bathylagus pacificus[a]	9681	176843	40–220	5100	185572	52–206	73
Bathymaster sp.	3	NA	37–39	0	0	NA	NA
Benthalbella dentata[a]	11	471	115–221	3	70	125–198	253
Berryteuthis anonychus[a]	6	78	NA	40	549	64–82	102
Berryteuthis magister[a]	437	13733	19–320	522	45121	17–305	108
Bothrocara brunneum[a]	9	419	121–325	11	566	106–362	58
Chauliodus macouni (sloani)[a]	63	2897	10–310	132	6868	82–279	130
Chiroteuthis calyx[a]	14	2381	30–205	14	2199	84–198	85
Coryphaenoides acrolepis	2	2599	235, 250	0	0	NA	
Coryphaenoides cinereus	32	1042	23–160	112	15433	29–162	
Coryphaenoides pectoralis	1	1.6	29	0	0	NA	
Cyclothone atraria	0	0	NA	205	113	36–60	
Cyclothone microdon	12	NA	39–59	0	0	NA	
Cyclothone pseudopallida	83	78	37–59	0	0	NA	
Diaphus theta[a]	152	1930	68–105	171	2412	71–105	290
Elassadon tremibundus	2	343	265–305	0	0	NA	
Eogonatus tinro[a]	593	16005	27–275	1301	35053	27–253	160
Galiteuthis phyllura[a]	25	216	47–300	131	2276	55–372	84
Gonatopsis borealis[a]	996	50545	23–165	934	42292	26–122	86
Gonatus berryi[a]	75	2552	28–215	74	3021	32–235	120
Gonatus madokai	0	0	NA	1	NA	550	
Gonatus middendorffi	1	NA	460	4	76	73–124	
Gonatus sppZ (2 types)	85	4849	53–195	126	6360	49–212	
Gonatus onyx	142	526	32–76	610	4008	27–125	
Gonatus pyros	108	798	29–168	392	2112	22–102	
Holtbyrnia innesi	0	0	NA	3	58	74–180	
Japatella diaphana	0	0	NA	6	710	52–125	
Japatella heathi	5	81	60–67	0	0	NA	
Lampanyctus jordani[a]	129	3610	97–143	250	6979	102–139	278
Lampetra tridentata	5	999	405–525	0	0	NA	
Lestidiops ringens	3	38	174–225	1	240	27	
Leuroglossus schmidti[a]	91943	610631	29–157	59172	511758	28–152	187
Lipolagus ochotensis[a]	450	4599	74–136	200	2013	64–146	150
Lycodapus fierasfer[a]	126	653	65–150	94	493	62–156	109
Lycodapus leptus	0	0	NA	NA	NA	NA	
Lycodapus poecilus	0	0	NA	27	175	44–146	
Lycodapus psarostomatus	0	0	NA	1	4	141	
Lycodapus sp	14	64	97–128	5	NA	51–65	
Macropinna microstoma[a]	12	218	51–140	16	421	72–139	100
Maulisia agripalla	0	0	NA	1	45	162	
Melamphaes lugubris[a]	79	1376	70–109	110	1818	68–98	365
Nannobrachium regale[a]	57	2045	97–190	37	1155	88–196	182
Nansenia candida[a]	1	81	227	1	73	220	249
Nectoliparis pelagicus	0	0	NA	1	1	56	
Oneirodes bulbosus	7	421	50–108	2	81	56–80	
Oneirodes thompsonii[a]	10	987	62–160	1	182	118	76
Opisthoteuthis californica	1	NA	NA	0	0	NA	
Paraliparis sp	1	24	183	0	0	NA	
Paraliparis dactylosus	0	0	NA	1	2	81	
Paraliparis paucidens	0	0	NA	10	150	97–210	
Paraliparis pectoralis	0	0	NA	1	8	119	
Pleurogrammus monoptergyius	0	0	NA	3	241	171–193	
Poromitra crassiceps[a]	228	5863	72–131	592	15386	84–135	212
Protomyctophum thompsonii[a]	12	35	48–58	106	229	36–60	142
Sagamichthys abei	1	43	166	0	0	NA	
Scopelosaurus harryi[a]	5	290	185–272	2	150	238,258	135
Sebastes alutus	2	NA	295,340	0	0	NA	
Sigmops (Gonastoma) gracilis[a]	11	71	114–143	36	250	113–160	
Stenobrachius leucopsarus[a]	9946	55147	33–115	25817	120895	29–120	222
Stenobrachius nannochir[a]	3541	33396	41–130	8703	56469	31–126	224
Tactostoma macropus[a]	5	70	125–245	7	624	202–370	156
Taonius borealis[a]	22	1695	110–482	40	2630	98–368	88
Tarletonbeania crenularis	4	10	58–61	1	2	59	
Vampyroteuthis infernalis	0	0	NA	1	11	33	

[a] Species included in energetic map analyses.

study (Table 1). *Stenobrachius leucopsarus* more than doubled in catch number and biomass between 1999 and 2000, a result that had been anticipated since twice as many hauls were conducted in the second year of study.

Despite the increase in absolute biomass in 2000 due to doubling of the haul effort, the predicted mass per haul decreased for many species in the observations both '*in situ*' and when averaged across the expanded study area, including for the dominant bathylagid and myctophid fish families. This is generally consistent with the fitted day/night vertical distribution, shown for selected species in the left columns of Figs. 3–5. Here, the fitted values are averaged across the extended study area, not just the haul locations, and units are the expected mass per haul based on species response to habitat conditions. The reduction in predicted biomass density in 2000 included the dominant myctophids *S. leucopsarus* and *D. theta* (Fig. 3) and all the bathylagids (except for *Psuedobathylagus milleri*, which increased in hauls at 500 m and 1000 m depths) (Fig. 4). In contrast, the predicted average mass per haul increased at all depths for *G. borealis* in 2000 relative to 1999 (Fig. 5a) when averaged across the study area, indicating favorable habitat characteristics outside the haul locations. Among the other dominant species of gonatids, *B. magister* predicted catch weights per haul remained the same between years (Fig. 5c), and *Gonatus berryi* decreased at all depths in 2000 (Fig. 5d). Most commonly, diel signals in mesopelagic vertical migration indicate an increase in predicted intra-specific mass at depth during night as compared to day (cf. Vecchione et al., 2015) – and that was the case in this study. However, some species exhibited a variable day/night response with depth (*D. theta*, Fig. 3c), greater biomass at all depths during the day (*G. borealis,* Fig. 5a), or only a weak D/N response (*E. tinro*, Fig. 5b; *S. nannochir*, Fig. 3b; *Lampanyctus jordani*, Fig. 3d) all of which may reflect intra-specific age-related patterns, reverse vertical migration, or no active vertical migration through the water column at all.

3.1.2. Community composition, species guilds, and habitat responses

Diel community composition at depth for both years combined is described by a cluster dendrogram of 14 species that occurred at a minimum of 75 individuals in each year of study (Fig. 6; Table 1). The original list of 30 species was maintained for all other modeling efforts, but reduced for cluster analyses in order to eliminate poorly represented species and ease interpretation for the vertical migration and habitat response patterns. Eleven of the 14 selected species fell within the 3 primary families represented in the study. The species most commonly and abundantly represented at each fishing depth during day and night generally clustered as expected based on observations in both field and laboratory in this and earlier records (*see*: Mecklenburg et al., 2002). Clusters of Day/Night (D/N) communities by vertical distributions (Fig. 6) are as follows: lower mesopelagic migratory 1000 m–500 m – (*Melamphaes lugubris – B. pacificus*); non-migratory at 1000 m (*Poromitra crassiceps*); and upper mesopelagic mostly migratory 500 m–250 m (*S. leucopsarus – E. tinro*). The latter guild comprises the greatest number of species and may be somewhat clouded by the variable migration patterns of different intra-specific age classes represented in the samples. Nonetheless, based on the limited amount of information available through direct collection of mesopelagic fish and squid species, as well as predator diet studies, many of the species one should expect to occur together in hauls at depth, by day or night in the fishing area are accurately indicated as clustered groups. The consistency of species' fitted vertical distributions with general expectations (particularly those known to reside only at 500 m or 1000 m depths) provides confidence that the sampling in this study is sufficient to effectively capture signals of habitat response, despite the use of an open net (Fig. 6).

Alternately, the same 14 species cluster according to their response to physical/biological (horizontal) habitat covariates, rather than day/night vertical distribution (Fig. 7). In this dendrogram we see a different grouping, with a greater number of guilds when compared to species guilds defined by vertical distribution. The first guild is comprised of two myctophids (*S. nannochir* and *D. theta)* and a bathylagid (*Lipolagus ochotensis*). *Diaphus theta* and *L. ochotensis* were closely associated by nature of their diel depth distribution patterns (Fig. 6) and each are additionally bound along with *S. nannochir*, by their strong negative association to increasing FSLE magnitudes; i.e., towards increased frontal activity (Table 2; Figs. 3 and 4). Of the 30 species evaluated, they are the only ones to respond in this sense to FSLE (Table 2). In addition, *D. theta* and *L. ochotensis* also respectively demonstrate a strong and moderately negative response to increasing GCS, which is elevated along fronts or around eddy perimeters (Table 2; Figs. 3 and 4). All other species registering any response to increasing GCS have a positive association (Table 2). The response to these two habitat covariates indicate that the *S. nannochir/L. ochotensis/D. theta* guild (*SDL*) would be predicted to occur at lower mass in areas of high frontal or eddy activity.

In the second guild, *L. schmidti* and *G. berryi* exhibited similar, structured, or mixed responses to both frontal variables (DTF and FSLE), and mixed or negative (*L. schmidti*) responses to SST (Table 2). The third guild (*S. leucopsarus-M. lugubris*) is the least consistent among the clustering in terms of habitat variable selection and response (Table 2), though *E. tinro* and *M. lugubris* both responded to SSTa, albeit in alternate senses, and GCS as predictors of mass. *Poromitra crassiceps* was the only species to exhibit responses to both chlorophyll and SSTa (Table 2).

Gonatopsis borealis and *B. magister*, two gonatid species, exhibited nearly identical responses to GCS and SLA (Fig. 5e, g) and likewise were clustered closely in their habitat response. The distribution by mass for each of these two species is equal at all depths when habitat response is applied to modeled vertical distribution D/N across the study area (Fig. 5a, c). One potential complication in interpreting these patterns is that the two species present multiple age classes in the sample, which is discussed further in the following section. *Lampanyctus jordani*, in an adjacent guild, exhibited similar responses to GCS and SST, but with an additional mixed response to chlorophyll and no response to SLA (Fig. 3h). *Lycodapus fierasfer*, in its own guild, had the same variable selection as *S. leucopsaurus*, but with a response to chlorophyll in the opposite sense (Table 2). *Lycodapus fierasfer* and *P. crassiceps* were two species that fell within their own independent guilds regardless of whether clusters were determined by vertical distribution or habitat response. For *P. crassiceps*, this result is likely related to their exclusive occurrence in only – and in all – eleven of the 1000 m hauls conducted in both years of study. In comparison, *L. fierasfer* occurred in 6 of the 1000 m hauls and in one additional haul at 250 m – the latter a single individual likely retained in the net from depth.

GCS was the most consistently selected of all habitat variables that were evaluated – particularly among the cephalopods (Table 2). Of the 7 species of cephalopods that were evaluated, all but *Gonatus berryi* demonstrated strong positive responses to GCS. Overall, the dominant species with positive response to increasing current speeds had higher average mass predictions in 2000. This was the case for the dominant gonatid squids in the sample – however, *B. magister* was the exception among these in that average predicted mass between years stayed the same (Table 2; Fig. 5c). The strong positive response to GCS by *B. magister* may have been tempered by the species mixed response to FSLE, with greatest response in the moderate category. One interpretation is that *B. magister* may prefer habitat within the linear BSC or ANSC (generally, high GCS, low/moderate FSLE), rather than in filaments or meandering flow (high GCS, high FSLE). As noted above, another possibility is that there may be a mix of age classes in the sample that require different habitat characteristics.

With the exception of those species demonstrating strong association with eddy activity and fronts (such as strong positive response to

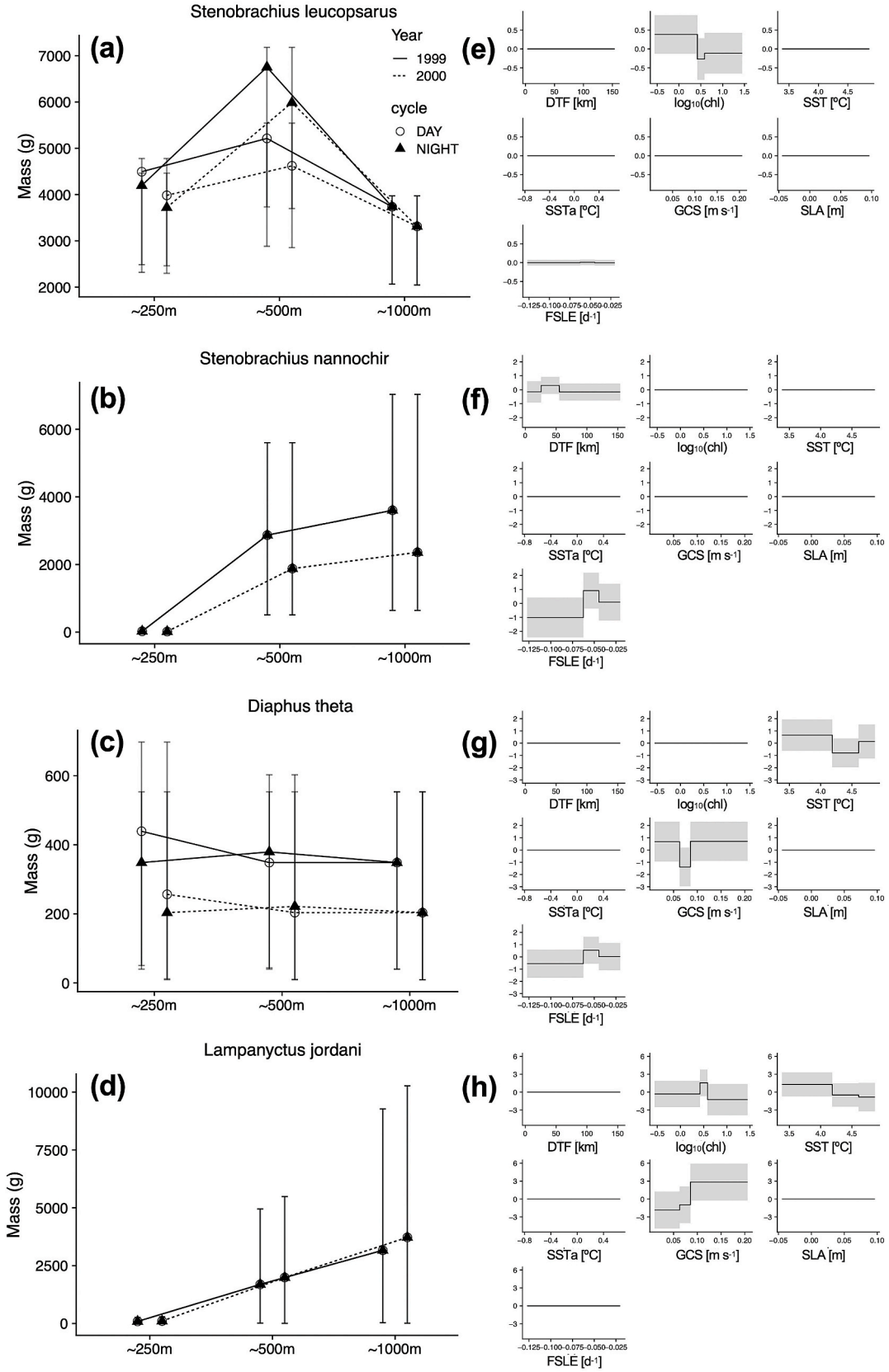

Fig. 3. The modeled (a–d) relative abundance at depth and (e–h) response to habitat variables by 4 species of fish from the family Myctophidae that dominate mesopelagic hauls and predator diets in the eastern Bering Sea Basin. The vertical migration plots represent predictions over the expanded study area. Bars represent the range of predicted mass (units: expected mass per haul). The habitat plots show the effect of each habitat covariate on predicted haul mass; flat lines indicate covariates not selected due to the regularization constraint on fitted GLMs. DTF: distance to front, chl: chlorophyll-*a*, SST: sea surface temperature, SSTa: SST anomaly, GCS: geostrophic current speed, SLA: sea level anomaly, FSLE: finite space Lyapunov exponent.

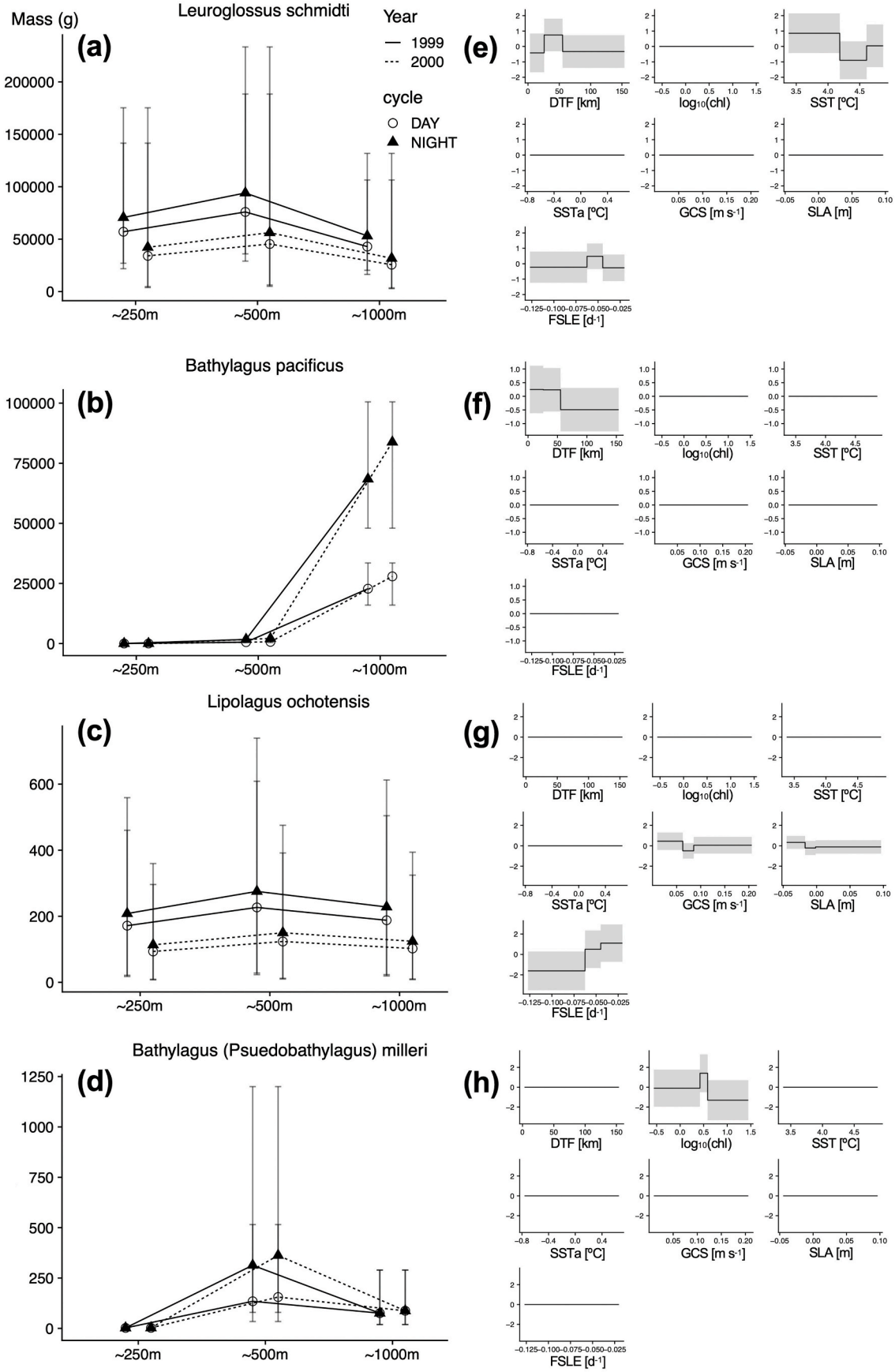

Fig. 4. As in Fig. 3 but for 4 species of fish from the family Bathylagidae that dominate mesopelagic hauls and predator diets in the eastern Bering Sea Basin.

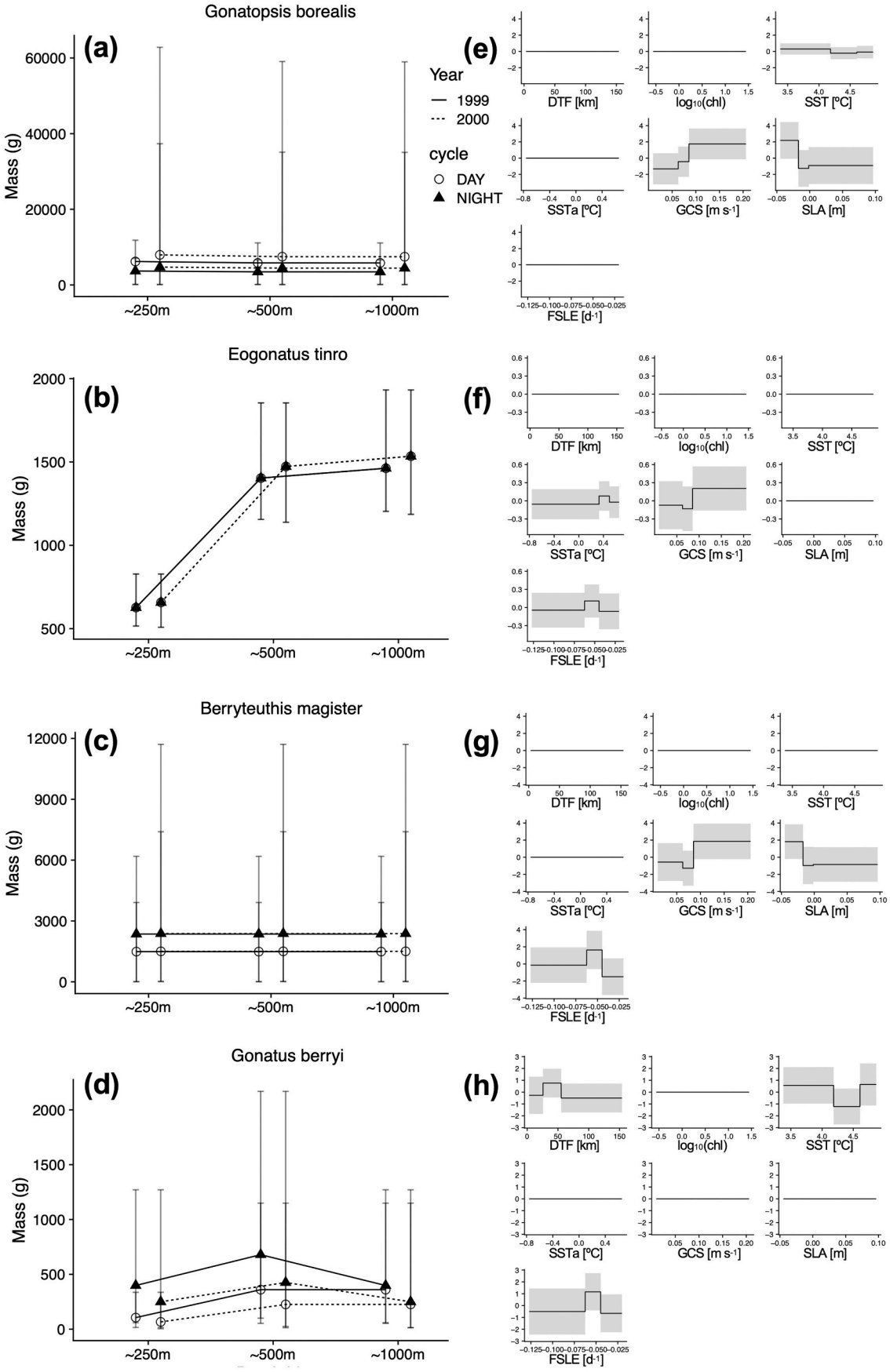

Fig. 5. As in Fig. 3 but for 4 species of squid from the family Gonatidae that dominate mesopelagic hauls and predator diets in the eastern Bering Sea Basin.

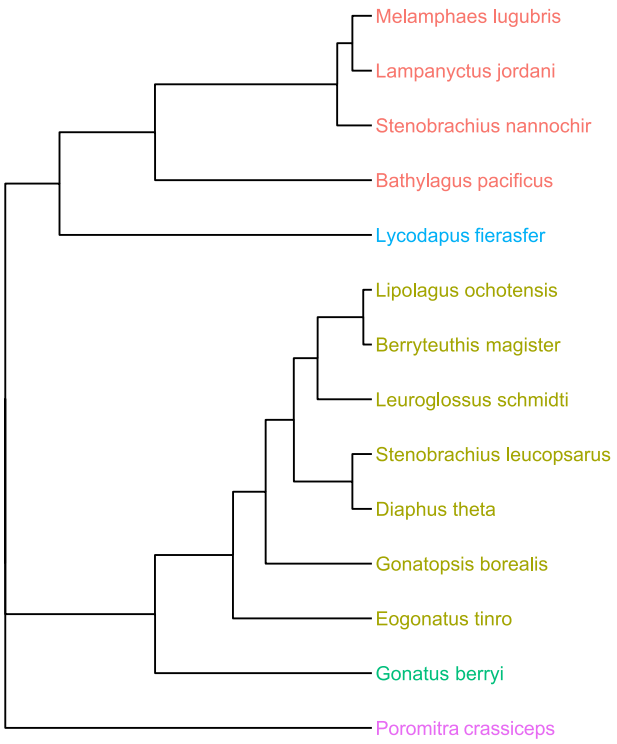

Fig. 6. The community composition (species guilds) based on clustering of vertical migration.

increasing GCS), and/or strong responses to moderate chlorophyll concentrations (Figs. 3h and 4h) the average species mass predictions across the expanded study area suggests that habitat conditions for many were more favorable in 1999 than in 2000 (Fig. 3a–c; 4a, 4c, 5 d).

3.2. Physics - a comparison between study years and locations

The sampling took place in two years of below-average mesoscale activity, as measured by eddy kinetic energy (EKE) within the expanded study area, with 1999 having the second-lowest value within the period 1993–2018 (Fig. 1b). The year differences in EKE are consistent with the categorical covariates related to mesoscale flow, with 2000 having more extensive regions of high geostrophic current speed, more frontal activity (elevated FSLE values), and smaller distances to the nearest front (Figs. 8 and 9). As noted previously, sea surface temperatures in the expanded study area were colder-than-average in 1999 and near-average in 2000 (Fig. 1c). These differences are driven in particular by elevated SST in the eastern half of the study area in 2000 (Figs. 8 and 9).

Flow in both the ANSC and BSC was stronger in May 2000 as compared to 1999 (Fig. 1a and b, 10). The typically meandering and eddy-rich nature of the BSC is apparent in both of these years (Fig. 1b). In 1999, a large eddy dipole centered at 193°W was embedded in the Alaska Stream – the strong western boundary current of the Gulf of Alaska found south of the Aleutian Islands – with weaker flow downstream of this (Figs. 1a and 10) and a weaker ANSC (*cf*. Stabeno and Hristova, 2014). In May 2000, the Alaska Stream was stronger and more continuous, and a defined ANSC was evident north of Samalga Pass (Figs. 1a and 10).

In 2000, some sampling occurred at the offshore-flowing edge of a meander in southeast portion of the basin, along the stretch of continental slope between Bering Canyon and Pribilof Canyon (Fig. 10b). The largest perturbation to the BSC flow in 1999 was instead an anticyclonic eddy centered southwest of Pribilof Canyon (Sinclair and Stabeno, 2002, Fig. 10). Composite chlorophyll concentrations were lower in the canyon and eddy center in this year, in contrast to concentrations within the linear BSC flow offshore of the canyon in 2000 (Figs. 8–10).

3.3. Energetics at depth across the expanded study

A total of 1495 individual fishes (n = 1184) and squids (n = 311) from 30 of the 72 species profiled were measured for their proximate composition (fats, proteins) and resulting energetic density (cal/100 g) (Table 1; *see* Sinclair et al., 2015). Discrete energetic values at age/size were available for only five of the 30 species so average intraspecific values were applied to all in this analysis. Using the mean energetic values per unit mass for each species, the fitted vertical and horizontal distributions of mass described above were converted to estimates of energy and summed across species to provide 3-dimensional maps of the relative mesopelagic energy content across the expanded study area in May of each year. These maps provide an illustration of how species-specific and guild responses to selected habitat variables at depth are manifested in the total estimated mesopelagic energy content (Figs. 11 and 12).

While energetic value can vary with collection location, season, age class and reproductive condition of the specimen, myctophids typically rank among the highest in proximate composition of both protein and fat and are subsequently among the most calorie rich of micronektonic schooling fishes and cephalopods (Sinclair et al., 2015, 2016). Of the three dominant family groups in this study, myctophid energetic values ranged from 142 to 290 cal/100 g, the bathylagids ranged 66–187 cal/100 g, and the gonatids 70–160 cal/100 g (Table 1).

Energy maps are shown in a relative sense, using an energy index scaled from 0 to 1 based on the maximum predicted total value across the expanded study area in either year (Figs. 11 and 12) rather than in absolute areal concentrations. This reflects the fact that models for mass were fit to 'per-haul' rather than areal units. A 'per haul' approach was selected due to our limited understanding at the start, of what defined a community (guilds) or the bounds of individual species distributions. For this reason, each haul was treated as its own community and the relationship between hauls was defined by modeled parameters. The use of a 'scale of probability' of energy value (a reflection of predicted mass) was a way of leveling out large differences in energy values and biomass between species so that the data could be more easily interpreted.

The most notable feature of the maps is their provision of annual snapshots of the dominant habitat features and associated response to those features (negative or positive) by both the dominant species (those with the greatest average weights/haul) and species guilds (additive mass). For instance, the highest levels of total energy index in 1999 occur in the north, south central and southwest portions of the expanded study area (Fig. 11). These high energy hotspots take the 'shape' reflected by high levels of physical activity within habitat boundaries defined primarily by the physical covariates DTF and FSLE, and (to a lesser degree) GCS in 1999 (Fig. 8). This aligns with our observations that many species had a strong positive response to an increasing geostrophic current (Table 2) and that, *B. pacificus*, the second most dominant species in total catch weight had a strong negative response to increasing distances from the front (Table 2). Elevated energy values in the north, southwest, and south portions of the extended study area generally correspond to areas of overlap between the moderate FSLE and DTF categories (Fig. 8) – both of which were positive predictors of the most abundant species by occurrence and weight, *L. schmidti*.

In 2000, we see a similar pattern of the strength of influence of DTF in energy profiles. Here, 'the shape' of moderate DTF values (Fig. 9) is reflected in 'the shape' of highest energy values (Fig. 12). We can also see that energy index levels are low in closest proximity to the front as defined by the similarity in shapes (Figs. 9 and 12). Other frontal features, such as FSLE play a role in the shape of energy response in 2000, at some depths more than others. Geostrophic current speeds appear to take a lesser role in influencing energetic response patterns compared to 1999. Even though high GCS values are more prevalent throughout the expanded study area in 2000, their influence on energy structure is less

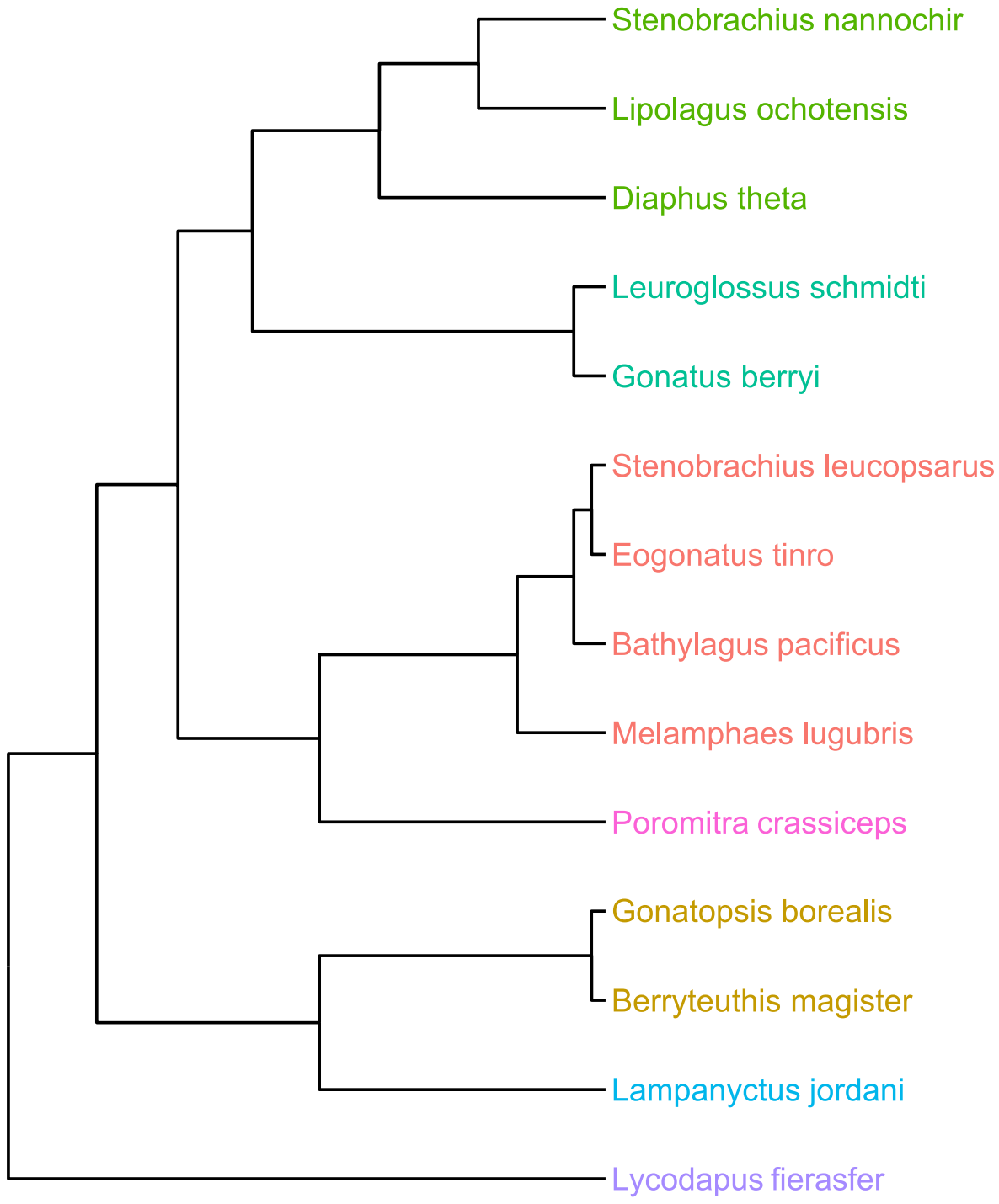

Fig. 7. The community composition (species guilds) based on clustering of habitat covariates.

apparent. This is likely because there is much less overlap between high-GCS, moderate FSLE, and moderate DTF regions in 2000 and high GCS species do not contribute as heavily to total energy. Overall, energy indices near the continental slope, in the southeast and northeast portions of the expanded study area, were predicted to be generally low in 2000 and high-energy areas confined to the interior of the basin, in contrast to 1999. The predicted total energy maps at 250 m depth in May for years other than those of our study (Fig. SI 3) similarly show large interannual differences in the presence of the highest energy indices and their location within the basin. These maps further illustrate how habitat relationships identified here have the potential to drive interannual variability in the spatial availability of mesopelagic species to surface based predators.

Those species that dominated haul weights and had a strong response (negative or positive) to habitat features characteristic of the year of study, were responsible for the greatest portion of the energy signature. This is the case even for those species that did not have appreciably high energy value (Bathylagidae); i.e., the catch weight signal more than compensated for the lower energy per unit mass of these species. Multi-species guild responses are certainly contributing to the total energy index levels, as is seen with geostrophic current, but individual species maps are even more dramatic in demonstrating the influence of habitat on species-specific distributions and the resulting level of their energy contributions across the greater basin. When examining the energy

Table 2
Species habitat response summary in GLMs for catch mass. Covariate responses are subjectively categorized for each species as being generally positive (+), negative (−), or neutral/mixed (~). Right-most column shows the number of effects used for each species. Covariate responses over all species are tallied at bottom. DTF: distance to front, chl: chlorophyll-*a*, SST: sea surface temperature, SSTa: SST anomaly, GCS, geostrophic current speed, SLA: sea level anomaly, FSLE: finite space Lyapunov exponent. The sign convention for FSLE is such that positive indicates increasing mass with increasing FSLE magnitude (greater frontal activity; *cf.* Figs. 3–5).

Species	DTF	$\log_{10}$(chl)	SST	SSTa	GCS	SLA	FSLE	# Effects Used
Bathylagus milleri		_						1
Bathylagus pacificus	_							1
Benthalbella dentata	~		_					2
Berryteuthis anonychus		~			+		~	3
Berryteuthis magister					+	_	+	3
Bothrocara brunneum				~	~			2
Chauliodis macouni		~	_		+		~	4
Chiroteuthis calyx		+	~		+			3
Eogonatus tinro				~	+		~	3
Diaphus theta			_		~		_	3
Galiteuthis phyllura		_	+		+			3
Gonatopsis borealis			_		+	_		3
Gonatus berryi	~		~				~	3
Lampanyctus jordani		_	_		+			3
Leuroglossus schmidti	~		_				~	3
Lipolagus ochotensis					_	_	_	3
Lycodapus fierasfer		+					~	2
Macropinna microstoma		+						1
Melamphaes lugubris				_	+	_		3
Nannobrachium regale			~		~			2
Nansenia candida								0
Oneirodes thompsoni	~	~	_					3
Poromitra crassiceps		+		_				2
Protomyctophum thompsoni		_			+			2
Scopelosaurus harryi								0
Sigmops gracilis	-		~					2
Stenobrachius leucopsarus		_					~	2
Stenobrachius nannochir	~						_	2
Tactosoma macropus					+			1
Taonius borealis		+						1

SUMMARY TALLY	DTF	$\log_{10}$(chl)	SST	SSTa	GCS	SLA	FSLE
# Any	7	13	12	4	15	4	11
# Positive	0	5	1	0	11	0	1
# Neutral	5	3	4	2	3	0	7
# Negative	2	5	7	2	1	4	3

distribution of each of three dominant species by mass (Figs. 13a–15d) it is evident that these have a dominant influence on the overall energy maps and 'shape' of energy concentrations for each year of study (Figs. 11 and 12).

Leuroglossus schmidti was found in habitat characterized by moderate distances to the nearest front, moderate FSLE values, and cool SSTs (Table 2; Figs. 4e, 8 and 9, 13). The overlap between these habitat categories had a major influence on the total energy maps in each year, as noted above. *Stenobrachius leucopsarus* demonstrates highest weights and energetic values in response to the singular habitat variable of low levels of chlorophyll (Table 2; Fig. 3e). In both years of study, *S. leucopsarus* energy patterns appear as an overlay of chlorophyll signature (Figs. 8, 9 and 14). The singular response of *B. pacificus* to distance to front, in conjunction with the high weight and strong presence of the species, also has an important influence on the overall energy maps, particularly in 1999 (Table 2; Figs. 4f, 8 and 9, 15).

4. Discussion

Sampling protocol was consistent between years and the increased number of trawls in 2000 was proportional to 1999 in terms of the relative number conducted at depth during day/night within the sampling year. Thus, the marked decrease in presence for a ubiquitous species like *L. schmidti* along with the entire bathylagid family of fishes suggests that a reduction in essential habitat requirements – or requirements for distribution of their prey may have occurred in 2000.

The use of a non-closing net likely resulted in unintended sampling of depths shallower than the targeted depth, however, we are encouraged by the well-defined patterns of species depth-specific presence as well as distinct species size-classes caught at specific depths. It seems that the duration and speed of tows and adjustments at net set and retrieval (per Russian researcher recommendations from decades of mid-water research; *see*: Sinclair and Stabeno, 2002) helped to reduce the effects of contamination between target depth layers. The sheer density of target species at their 'preferred' depth also helped to reduce the effects of contamination between depths.

In addition to the general patterns of species-specific depth occurrence with time of day, the implication that there was minimal contamination of bycatch between fishing layers is indicated by six species that demonstrated ontogenetic size distribution with depth. Species that occurred in two or more size categories distinguished by depth were *B. pacificus*, *S. leucopsarus*, *S. nannochir*, *G. borealis*, *Gonatus berryi* and *Berryteuthis magister*. For example, *B. pacificus* ranges primarily between 500 m and 1000 m depths with juvenile sizes occupying the shallowest portion of the range in 500 m tows (Fig. SI 4). While there is overlap in depth ranges of *B. pacificus*, the heavier adults tend to be caught in 500 m–1000 m tows. Ontogenetic migration has been identified in the literature for *B. magister* wherein juveniles reside in the upper levels of the water column dropping to deeper zones as they mature (*see*: Sinclair et al., 1999). This is a strategy that not only serves their life history and diet requirements, but – as has been shown for other species (i.e. walleye pollock, Dwyer et al., 1987) – serves to reduce their exposure to cannibalistic adults. For example, vertical migration patterns in our data demonstrate that *B. magister* and *G. borealis* are

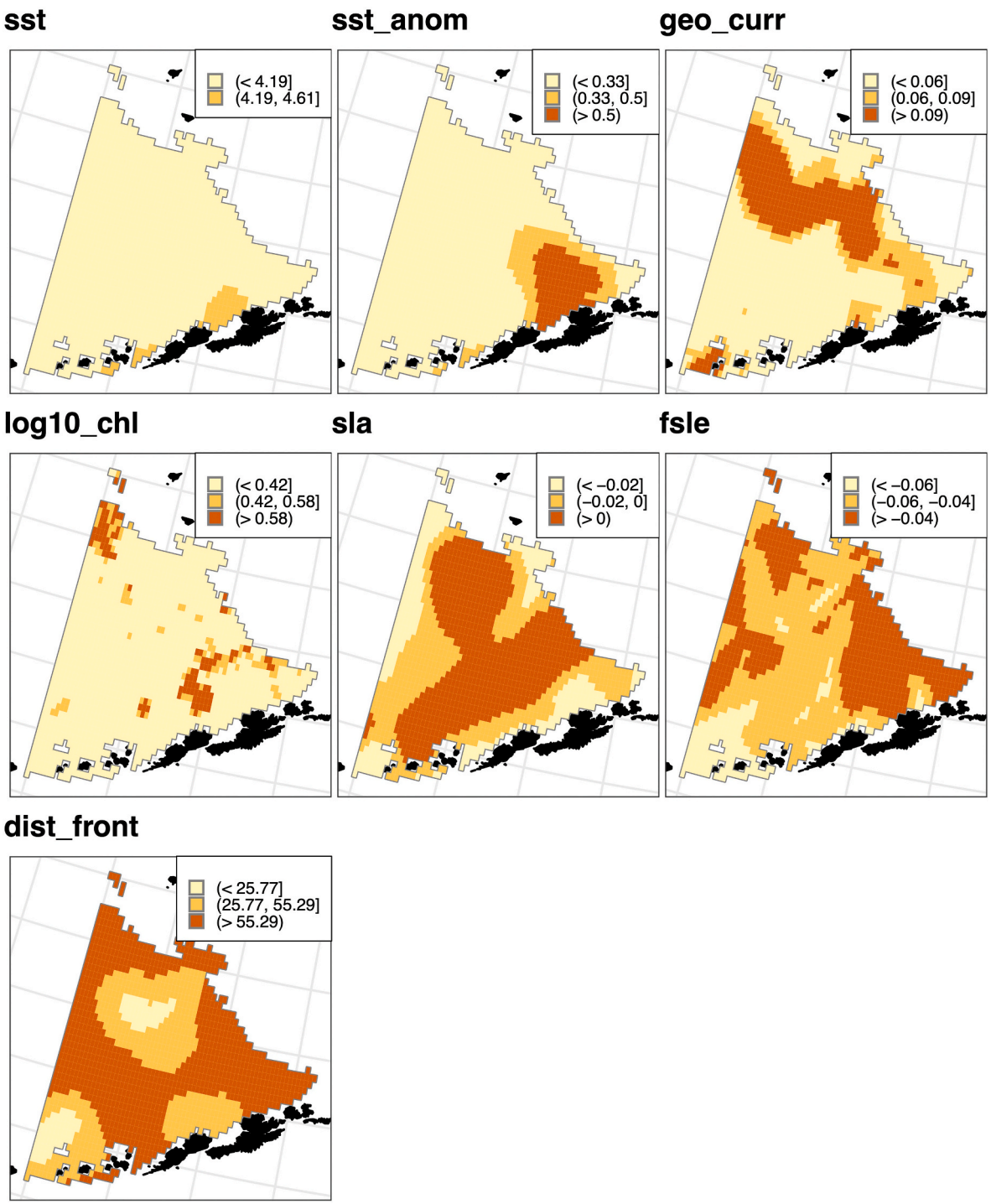

Fig. 8. Physical discretized co-variate values within the expanded study area, May 1999. sst: sea surface temperature, sst_anom: SST anomaly, geo_curr: geostrophic current speed, chl: chlorophyll-*a* sla: sea level anomaly, fsle: finite space Lyapunov exponent, dist_front: distance to front. Covariates have been classified into three categories based on the distribution of the values interpolated to hauls in May 1999–2000 (*see*: Methods).

equally present day and night at all three depth categories (Fig. 5a, c). In reality, at least two sets of size distinctions and migratory activities are in play, with adult sizes caught between 500 m–1000 m, while juveniles were caught at 250 m as the lower boundary of their distribution (Sinclair and Stabeno, 2002) and likely migrating into the epi-pelagic at night. Based on our first year of data, we know that *Berryteuthis magister* juveniles are twice as likely to be caught during the day at 250 m rather than the night (Sinclair and Stabeno, 2002). The same may be indicated by the suggestion in this study of a higher mass of *G. borealis* at all depths during day than at night (Fig. 5e). The only other species to clearly demonstrate what at first glance appears to be a reverse diel migration pattern was *Diaphus theta* where mass at 250 m during the day is higher than at night (Fig. 3c). Age-related body lengths were not immediately observable in the raw data due to the small length range of *D. theta* (Table 1) and, as is the case with most of the species evaluated here, there is insufficient knowledge of species-specific age-related growth.

The energy index maps provide a 3-dimensional view of energy dispersal throughout the greater Bering Sea Basin. In addition to the latitudinal and longitudinal patterns they demonstrate the vertical extent of energy 'hotspots' in the water column due to species vertical

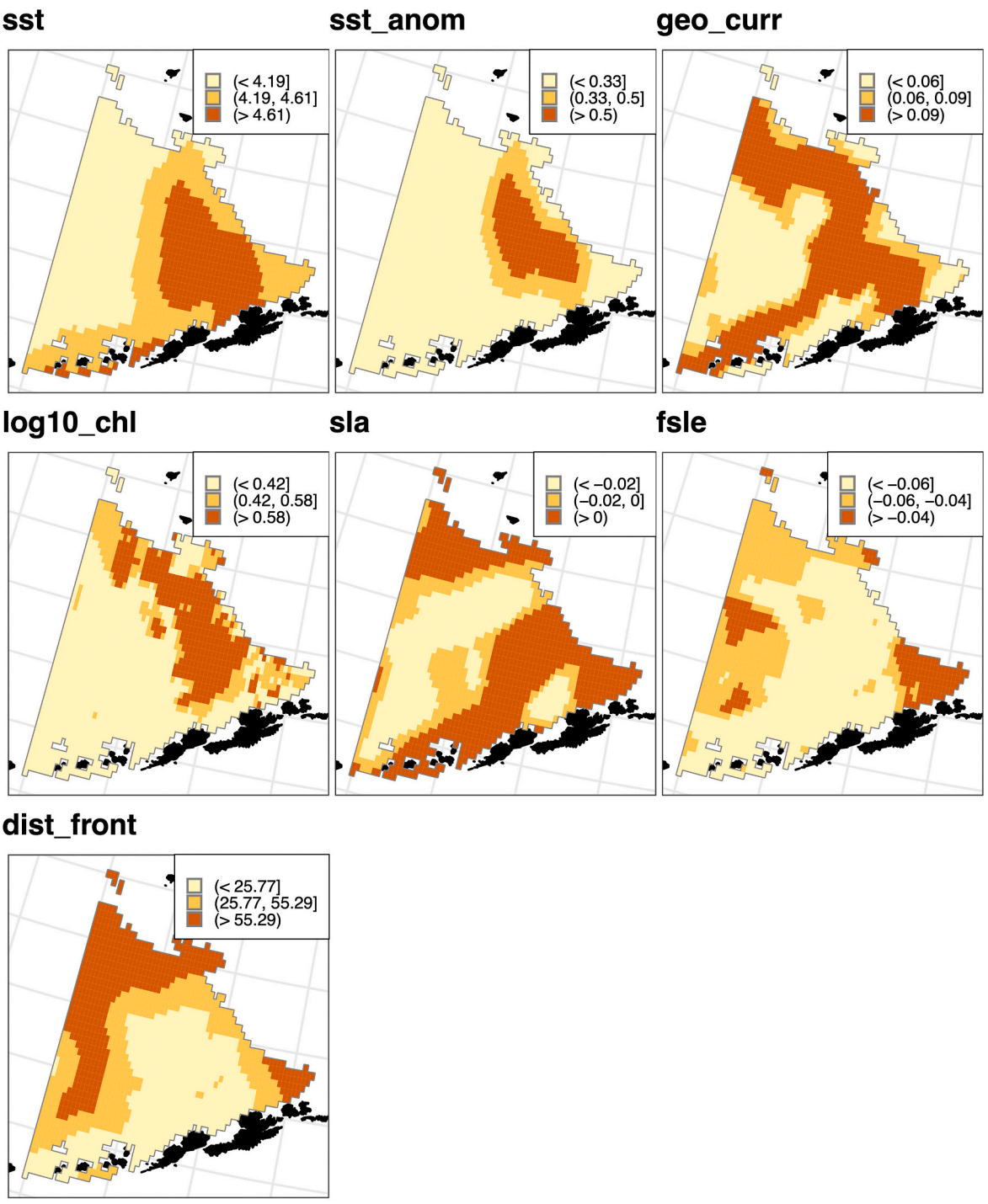

Fig. 9. As in Fig. 8, for the expanded study area, May 2000.

migration (Figs. 11 and 12). Note that different predator species accessing the EBS Basin may have differing depth ranges, prey capture abilities, energetic requirements, behavioral constraints (i.e., central-place foraging due to nursing a dependent offspring), or other factors, and not all predators can access all components of the energy maps shown in this study. Primarily, the maps are presented as an illustration of the ways in which the habitat relationships identified in this study have the potential to drive spatially heterogeneous, highly interannually variable prey availability (Fig. SI 3), whose ecological sources and implications for specific predators warrants further study.

Age-related patterns in the D/N distributions of fishes and squids clearly affect interpretation of energy values at depth as adults are frequently more energy rich than juveniles (Sinclair et al., 2015). While age/size patterns were observable with depth and confirmed in analyses, there is limited energetic information available on micronektonic species age/size associated energy values. This lack of information along with the large volume of data inherent to this study meant that intra-specific 'age/size classes' and their associated energy values were by necessity averaged for calculations of presence and biomass. Only 5 of the 30 species evaluated had available breakdown of energy at age/size and of the 3 species driving large scale energetic patterns only *S. leucopsarus* had age-energy information that fell within size ranges of this study. Although fine scale information was lost due to these limitations we are confident that the analyses in addition to the tabulated

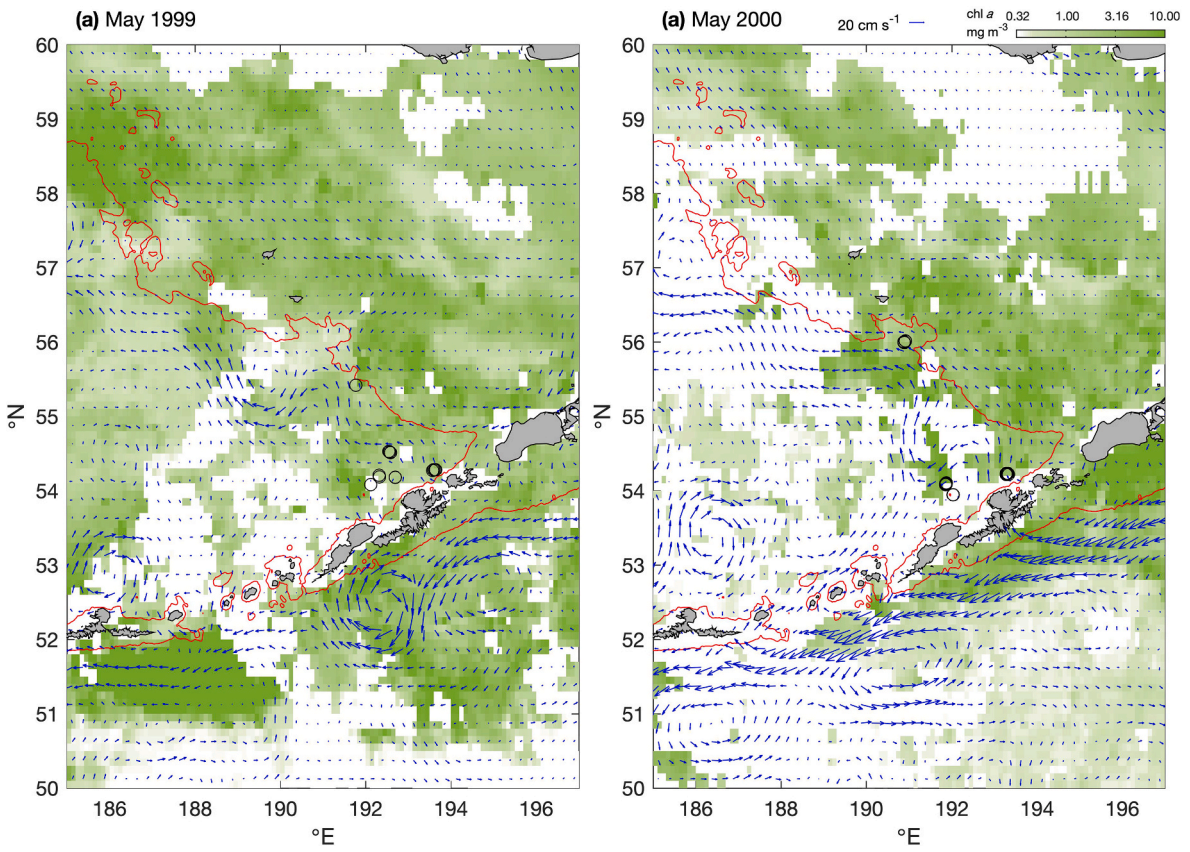

Fig. 10. Surface chlorophyll-*a* and geostrophic currents, plotted as in Fig. 1, observed during the month of sampling in each year of study, (a) 1999 and (b) 2000.

information provided will be useful in future to those identifying the physical parameters that influence species life history habitat boundaries and the foraging strategies of predators that select prey according body size (and thus, energy at a finer scale) and location in the water column (Sinclair et al., 1994, 2015).

Large scale observations of the deep scattering layer across ocean basins suggest that primary productivity is an important predictor of acoustic backscattering intensity and likely, biomass (Proud et al., 2017). However, the results of this study are consistent with the findings of other recent work indicating that, at smaller scales, such effects are superimposed on potentially larger effects of physical structure and dynamic processes that shape the mesopelagic prey field (Della Penna and Gaube, 2020). Here, while surface chlorophyll – a key input for parameterizations of productivity – was selected as a predictor for one of the three most abundant species, the sense of this relationship was towards low abundance at high chlorophyll (*S. leucopsaurus*, Fig. 3e). Among all major species sampled, while chlorophyll was selected as a predictor almost as often as GCS, the response type was evenly distributed between positive, negative, and mixed (Table 2). Because the regularization constraint imposed in GLM fitting is intended to eliminate covariates that are not contributing to the model fit, we believe the results imply a real effect on catch weight in our samples, but it is possible that either the biological reasons for these relationships are indirect, or chlorophyll is correlated with an additional biological driver that is not present in our covariate set. For negative responses to chlorophyll, indirect biological reasons could relate to predator avoidance, or prey species abundance negatively correlating with chlorophyll (Fernandes et al., 2012). While it is beyond the scope of this paper to identify distinct ecological drivers for each species habitat relationship found here, small-scale relationships between midwater biomass and chlorophyll or productivity at the sea surface do not appear to be straightforward in this and other ecosystems (Saijo et al., 2017; Della Penna and Gaube, 2020).

The vertical scales of major currents and mesoscale features in the southeastern Bering Sea can reach from the surface to 500–1000 m or greater (Kinder et al., 1975; Roden, 1995; Cokelet and Stabeno, 1997; Chen and Firing, 2006; Mizobata et al., 2006) and therefore surface physical signatures can be indicative of processes that may be directly impacting the depth levels that were sampled in this study. As well, the vertical migration and use of surface habitat of many mesopelagic species suggests that surface characteristics could plausibly influence their presence or concentration at depth. However, as noted previously, it should be acknowledged that surface features alone do not encompass the entirety of habitat processes that may be important to mesopelagic fishes and squids and their use for prediction is necessarily a compromise. Notably, surface features lack information on the concentration of dissolved oxygen at depth, which is an important constraint on mesopelagic habitat (Ekau, 2010; Sutton et al., 2017); climatological oxygen (Panteleev et al., 2013) was considered as a predictor in this study, but it was indistinguishable from depth when converted to a categorical variable. Indeed, there is evidence from other regions that the ability to distinguish the mesopelagic assemblage using surface oceanographic features alone decreases with increasing depth and, potentially, with increasing size or trophic level (Vecchione et al., 2015). Decreasing responses with depth were noted in hauls 750–1500 m depth and deeper in Vecchione et al. (2015); unfortunately, the observations in this study are not well-suited to test this hypothesis since two of three haul depths were shallower than this. The observation of an overall change in community structure with depth – implied by the differing depth structures across species in this study – is consistent with the results of Vecchione et al. (2015) for micronekton along the mid-Atlantic ridge.

One important contribution of this study is the ability to distinguish between a large number of species contributing to the mesopelagic assemblage, over a variety of locations, in two different years, in a

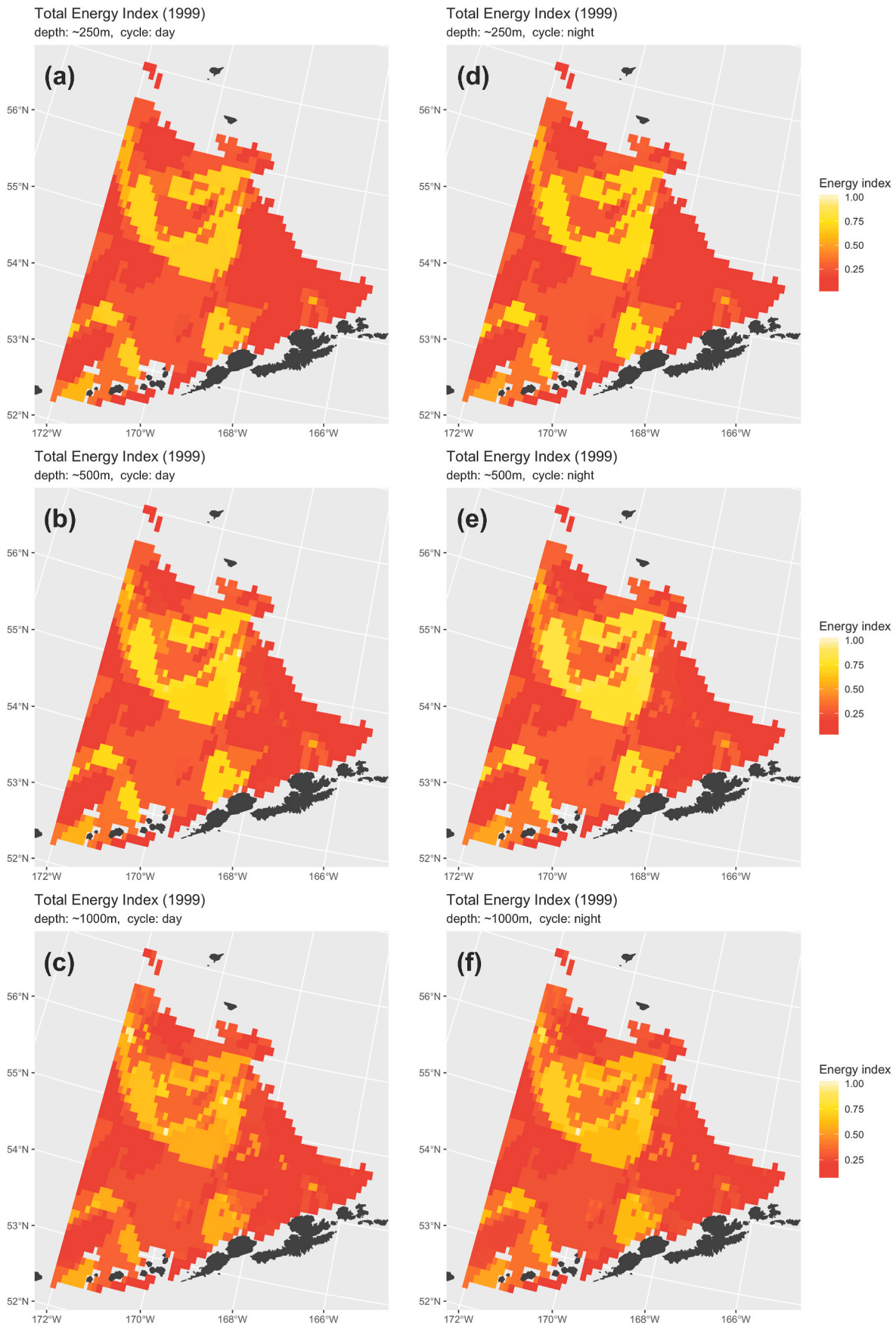

Fig. 11. Predicted total mesopelagic energy at three depths during day (a-c, left column) and night (d-f, right column) in the expanded study area in May 1999. Energy index values range from 0 to 1, where 1 indicates the highest predicted value at any location in 1999–2000.

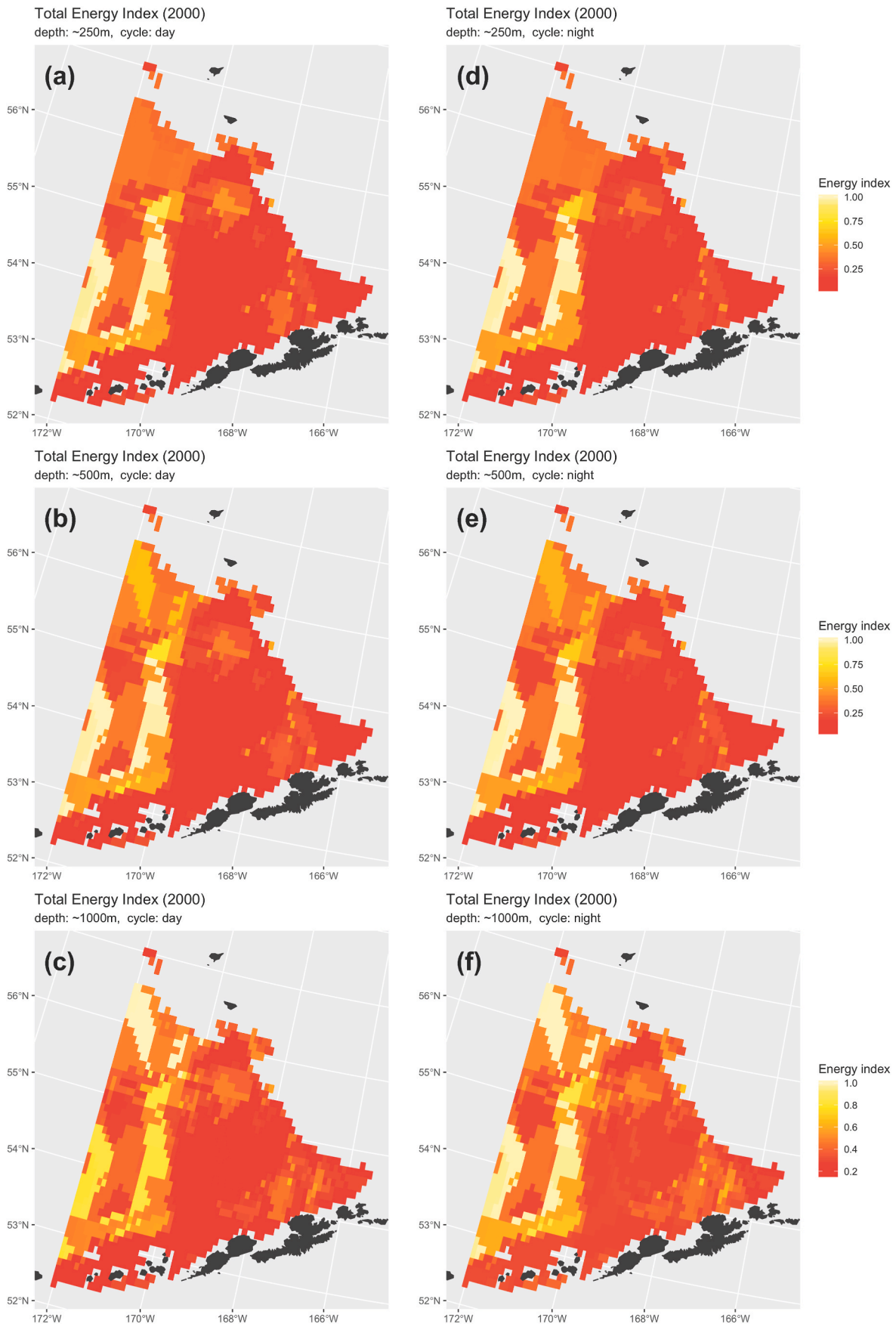

Fig. 12. Predicted total mesopelagic energy in the expanded study area in May 2000, plotted as in Fig. 11.

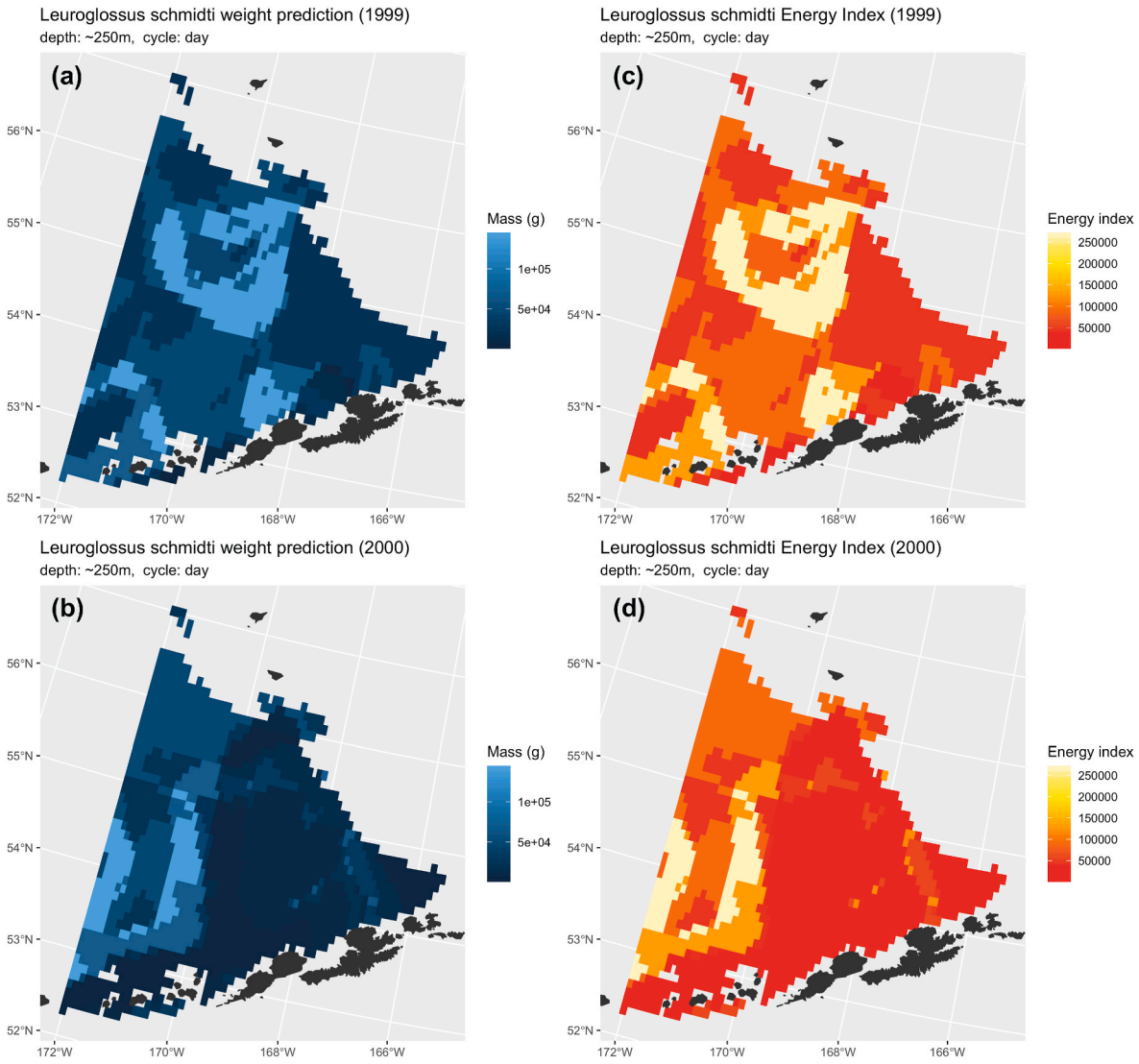

Fig. 13. The (a–b) weight predictions and (c–d) subsequent energy index values for *Leuroglossus schmidti* at 250 m during the daytime across the expanded study area in 1999 (a, c) and 2000 (b, d).

relatively under sampled subarctic ecosystem. Overall, the suite of responses to dynamic habitat covariates (Figs. 3–5, Table 2) provide evidence that the mesopelagic prey field in this ecosystem does not respond in homogeneous fashion to variation in physical and biological processes, though certain physical covariates do have more consistent signatures across species. Geostrophic current speed, chlorophyll, SST, and FSLEs were selected most often as predictors of relative abundance among the major species (Table 2). Each of these exhibited at least one species with each type of response (positive, negative, or mixed). However, of these, GCS had predominantly positive responses, while SST was predominantly negative. Chlorophyll was spread evenly as described above, and FSLE had a preponderance of mixed or neutrally structured responses. If such a result holds across the productive summer season, one hypothetical strategy for an opportunistic/generalist predator species would be to cue preferentially on covariates that produce the most consistent responses among the different mesopelagic species.

In the Bering Sea, there is both direct and indirect evidence that surface frontal features are capable of entraining and concentrating zooplankton, micronekton and ascending trophic levels of predators and, as such, presumably enabling efficient transfer of concentrated sources of energy to foraging marine mammals and birds (Sinclair et al., 1994; Antonelis et al., 1997; Beamish et al., 1999; *see*: Hunt et al., 2002; Sinclair et al., 2008; Sterling, 2009; Nordstrom et al., 2013). Here, the frequent selection of frontal variables suggests that these structures were influencing mesopelagic habitat selection, although not in a unidirectional sense. As noted above, the covariates used to predict abundance observed at depth in this study are entirely surface-based. Whether surface features further influence or concentrate mesopelagic species abundance during upward vertical migration – when mesopelagic species are more available to surface-based predators – cannot be fully addressed in this study but warrants continued investigation. It should also be noted that, although SLA was included as a covariate, coherent eddies, which are major features of the SE Bering Sea in some years (e.g., Cokelet and Stabeno, 1997; Mizobata and Saitoh, 2004) were not objectively identified or extensively sampled in this study. However, the selection of GCS as a positive predictor of mass in many species, particularly cephalopods as noted above, would be consistent with elevated biomass of these species at the periphery of eddies (Sinclair and Stabeno, 2002; *cf*. Sterling, 2009) where geostrophic currents are strongest and where apex predators may be likely to target their foraging effort. Horizontal and vertical boundary structures and the ability of predators to detect them are particularly relevant in the open ocean where prey resources are patchy. While eddies are among the most dynamic (Godø et al., 2012; Sterling, 2009) and proliferate

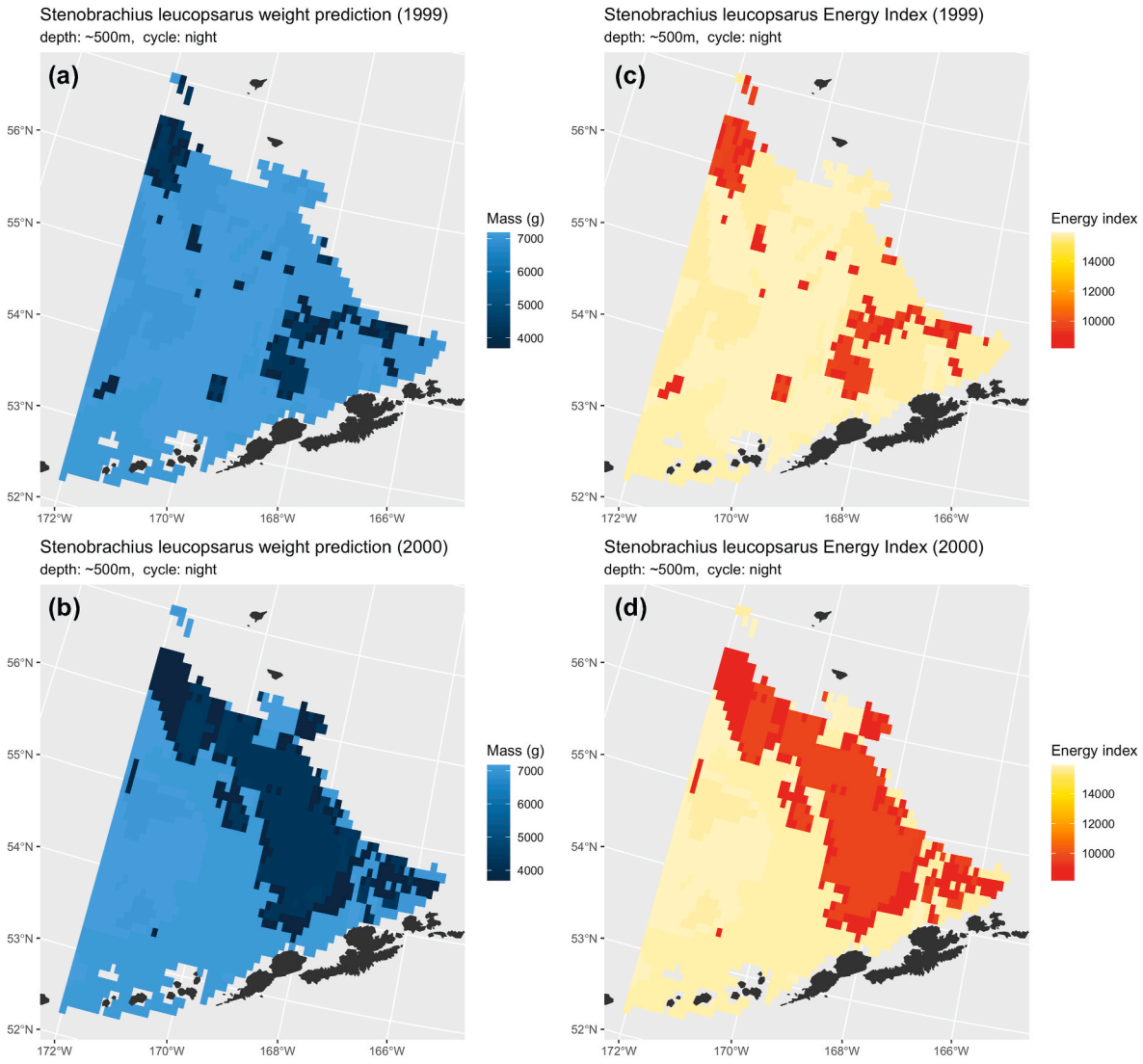

Fig. 14. The (a–b) weight predictions and (c–d) subsequent energy index values for *Stenobrachius leucopsarus* at 500 m during the nighttime across the expanded study area in 1999 (a, c) and 2000 (b, d).

concentrating mechanisms in the EBS Basin (Sinclair and Stabeno, 2002) our study shows that not all mesopelagic species respond in equal fashion to indicators of them.

Our description of the physical conditions in spring over a two year period demonstrates that species-specific distributions are highly localized by habitat response. This is a different consideration than the generalized view of a vertically migrating deep-scattering layer approaching the upper levels of the water column en-masse. For central-place foragers such as northern fur seals and marine birds that forage within a limited distance from rookery and nesting sites during late spring – summer months in the Bering Sea, differences in the spatial distribution of mesopelagic energy between years (*cf.* Figs. 11 and 12) may plausibly impact foraging energetics and efficiency as much as differences in overall integrated energy. The habitat redistributions predicted here provide a possible mechanism for interannual variations in predator habitat use, energy expenditure, and diet and ultimately reproductive success for those depending on a ready prey source in order to successfully raise pups and chicks onshore. Many fish and squid species identified strong negative or positive association with indicators associated with eddying flow, but neither study year demonstrated above average features of strong eddy activity. So how might predators detect prey in general, and specifically in years of low habitat indicators? Our evidence of inhomogeneity in how the mesopelagic responds to habitat variables has some interesting implications for predators of different species.

Habitat association by fishes and squids may have less to do with the direct physical requirements of a particular species and more to do with the physical requirements of the prey that they eat. As free-swimming animals that can travel great dimensional distances in a day, the physical habitat variables that mesopelagic micronekton associate with may be an indirect indication of the distribution of their food – some of which is subject to passive drift, stirring, and entrainment in boundary zones at fronts and in the interior of eddies. The predator-prey factor is part of the story of species multi-dimensional response to habitat variables that should be further evaluated.

5. Summary and conclusions

In this study, high-quality *in situ* sampling provides novel detail regarding environmental factors that have variable influences on species-specific distributions and biomass in the mesopelagic. Overall, our results indicate a complex and multifaceted relationship between physical/biological predictors for the total mesopelagic energy field during the spring bloom period in this highly productive ecosystem. Results are consistent with other recent findings that at sub-basin scales, physical variables become more important than lower trophic level

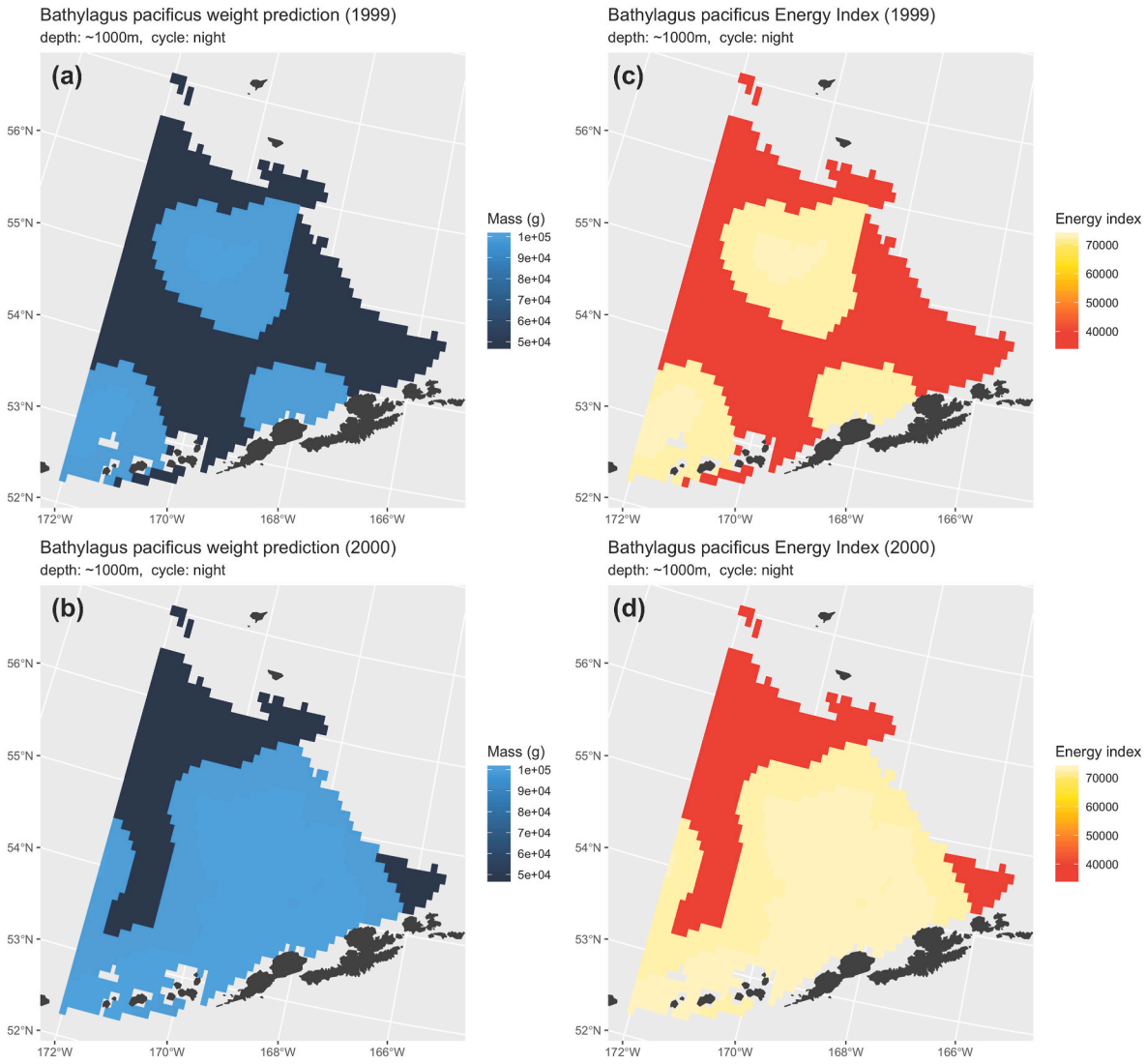

Fig. 15. The (a–b) weight predictions and (c–d) subsequent energy index values for *Bathylagus pacificus* at 1000 m during the nighttime across the expanded study area in 1999 (a, c) and 2000 (b, d).

activity in determining horizontal distributions of mesopelagic species. The three most abundant species show contrasts in the suite of physical and biological variables that they respond to, and also in the character of their response. While covariates related to the mesoscale flow field were important predictors for two of these species, the nature of the response was not unidirectional, with moderate rather than high or low values of frontal activity and distance to front associated with the highest response in the most abundant species (*L. schmidti*). This species also dominates the pelagic diets of a number of Bering Sea predators including the 'depleted' northern fur seal, and its availability as prey influences the population health of many others.

Among the most well-sampled species, guilds determined using *post hoc* clustering were generally consistent with classification of species behavior whose vertical distribution has been identified in earlier studies, giving confidence that the sampling was capable of capturing signals related to habitat response. Species clustered differently according to vertical distribution or response to surface habitat variables, with a greater number of guilds for surface habitat reflecting an inhomogeneous and diverse set of community responses. Nonetheless, some oceanographic variables were more consistent predictors than others, in particular sea surface temperature and geostrophic current speed, the latter particularly for cephalopod species. The precise mechanisms that account for these associations cannot be determined from the available data, but further research in this regard could inform whether the relationships determined here apply at other times of year or outside the Bering Sea ecosystem. Associations with geostrophic current speed and other variables related to mesoscale flow in the Bering Sea, which varies dramatically throughout the productive spring, summer, and autumn, provides a potential mechanism for meaningful variations within and between years in spatial distribution of mesopelagic prey at scales relevant to central-place foraging top predator species.

Declaration of competing interest

The authors declare that they have no known competing financial interests or personal relationships that could have appeared to influence the work reported in this paper.

Acknowledgements and Data Access Info

Field and lab support for this study was originally provided by the National Oceanic and Atmospheric Administration (NOAA) through the Fisheries-Oceanography Coordinated Investigations (FOCI) program and the Cooperative Institute for Arctic Research, a joint institute of NOAA and the University of Alaska Fairbanks. The study was completed with support from NOAA, National Marine Fisheries Service, Marine

Mammal Laboratory, Seattle, WA under contract number 1333MF19PNFFS0312. NAP was partially supported by the National Research Council Research Associate Program during this work. SeaWiFS and MODIS-Aqua surface chlorophyll *a* 9 km images were obtained from the NASA Ocean Color OPeNDAP server at https://oceandata.sci.gsfc.nasa.gov/opendap/SeaWiFS/L3SMI/and https://oceandata.sci.gsfc.nasa.gov/opendap/MODISA/L3SMI/. NOAA OISST V2 High-Resolution data were obtained from NOAA/OAR/ESRL PSD at https://www.esrl.noaa.gov/psd/data/gridded/data.noaa.oisst.v2.highres.html. The ETOPO1 data were obtained from the National Centers for Environmental Information/National Geophysical Data Center at https://www.ngdc.noaa.gov/mgg/global/. The gridded SLA and ADT SSALTO/DUACS altimeter products were produced and distributed by the Copernicus Marine and Environment Monitoring Service (http://www.marine.copernicus.eu). FSLE data were processed by SSALTO/DUACS and distributed by AVISO+ (https://www.aviso.altimetry.fr) with support from CNES.

Special acknowledgement to the crew of the now retired NOAA research vessel *Miller Freeman* for their pioneering efforts at obtaining quality haul samples, and to the late Dave King and team of the Sand Point Seattle NOAA/NMFS net loft for their duplication of the Russian cod-end netliner that changed the course of open-mouth net sampling at depth. Likewise, to the Alaska Fisheries Science Center field and lab 'meso' research team for their many hours of capable effort ensuring the success of this pilot study: Dennis Benjamen, Kate Call, Carolyn Kurle, Sigrid Salo, Phyllis Stabeno, Jim Thomason, Bill Walker and Tonya Zeppelin. This pilot study would not have advanced far beyond field efforts without Bill Walker's expertise and care in the identification and enumeration of the damaged and partial remains of delicate fishes and squids of the mesopelagic. We extend additional thanks to the Marine Mammal Laboratory food habits program and Jeremy Sterling who each graciously conferred with the authors regarding the relevance of these results to top predator species foraging in the Bering Sea. Janet Duffy-Anderson and Carey Kuhn provided helpful reviews of the manuscript.

Appendix A. Supplementary data

Supplementary data to this article can be found online at https://doi.org/10.1016/j.dsr.2022.103704.

References

Amante, C., Eakins, B.W., 2009. ETOPO1 1 Arc-Minute Global Relief Model: Procedures, Data Sources and Analysis. NOAA Technical Memorandum NESDIS NGDC-24. National Geophysical Data Center, NOAA. https://doi.org/10.7289/V5C8276M. (Accessed 11 January 2017).

Anderson, T.R., Martin, A.P., Lampitt, R.S., Trueman, C.N., Henson, S.A., Mayor, D.J., 2019. Quantifying carbon fluxes from primary production to mesopelagic fish using a simple food web model. ICES (Int. Counc. Explor. Sea) J. Mar. Sci. 76, 690–701.

Antonelis, G.A., Sinclair, E.H., Ream, R.R., Robson, B.W., 1997. Inter-island variation in the diet of female northern Fur seals (*Callorhinus ursinus*) in the Bering Sea. J. Zool., Lond. 242, 435–451.

Balanov, A.A., Il'inskii, E.N., 1992. Species Composition and Biomass of Mesopelagic Fishes in the Sea of Okhotsk and the Bering Sea. Scripta Technica, Inc. ISSN0032-9452/92/0004-0085.

Beamish, R.J., Leask, K.D., Ivanov, O.A., Balanov, A.A., Orlov, A.M., Sinclair, B., 1999. The ecology, distribution, and abundance of midwater fishes of the subarctic Pacific gyres. Prog. Oceanogr. 43, 399–r442.

Belkin, I.M., 2016. Comparative assessment of the west Bering Sea and east Bering Sea large marine ecosystems. Environmental development 17, 145–156.

Benoit-Bird, K.J., et al., 2013a. Foraging behavior of northern Fur seals closely matches the hierarchical patch scales of prey. Mar. Ecol. Prog. Ser. 479, 283–302.

Benoit-Bird, K.J., et al., 2013b. Prey patch patterns predict habitat use by top marine predators with diverse foraging strategies. PLoS One 8 (1), e53348.

Capotondi, A., et al., 2019. Observational needs supporting marine ecosystems modeling and forecasting: from the global ocean to regional and coastal systems. Front. Mar. Sci. 6, 623. https://doi.org/10.3389/fmars.2019.00623.

Chelton, D.B., Schlax, M.G., Samelson, R.M., 2011. Global observations of nonlinear mesoscale eddies. Prog. Oceanogr. 91 (2), 167–216.

Chen, S., Firing, E., 2006. Currents in the aleutian Basin and subarctic North pacific near the dateline in summer 1993. J. Geophys. Res.: Oceans 111 (C3).

Cokelet, E.D., Stabeno, P.J., 1997. Mooring observations of the thermal structure, salinity, and currents in the SE Bering Sea basin. J. Geophys. Res.: Oceans 102 (C10), 22947–22964.

Crawford, T.W., 1981. Vertebrate Prey of *Phocoenoides Dalli*, (Dall's Porpoise) Associated with the Japanese High Seas Salmon Fishery in the North Pacific Ocean. Msc thesis, University of Washington, Seattle, WA, p. 72.

d'Ovidio, F., Fernández, V., Hernández-García, E., López, C., 2004. Mixing structures in the Mediterranean Sea from finite-size Lyapunov exponents. Geophys. Res. Lett. 31 (17).

Della Penna, A., Gaube, P., 2020. Mesoscale eddies structure mesopelagic communities. Front. Mar. Sci. 7, 454. https://doi.org/10.3389/fmars.2020.00454.

Dunn, P.K., Smyth, G.K., 2005. Series evaluation of Tweedie exponential dispersion model densities. Stat. Comput. 15, 267–280.

Dwyer, D.A., Bailey, K.M., Livingston, P.A., 1987. Feeding habits and daily ration of walleye pollock (*Theragra chalcogramma*) in the eastern Bering Sea, with special reference to cannibalism. Can. J. Fish. Aquat. Sci. 44, 1972–1984.

Ekau, W., Auel, H., Pörtner, H.-O., Gilbert, D., 2010. Impacts of hypoxia on the structure and processes in pelagic communities (zooplankton, macro-invertebrates and fish). Biogeosciences 7 (5). https://doi.org/10.5194/bg-7-1669-2010.

Falkowski, P., Scholes, R.J., Boyle, E., Canadell, J., Canfield, D., Elser, J., Gruber, N., Hibbard, K., Hogberg, P., Linder, S., Mackenzie, F.T., Moore III, B., Pedersen, T., Rosenthal, Y., Seitzinger, S., Smetacek, V., Steffen, W., 2000. The global carbon cycle: a test of our knowledge of earth as a system. Science 290, 291–297.

Fernandes, L.D.A., Quintanilha, J., Monteiro-Ribas, W., Gonzalez-Rodriguez, E., Coutinho, R., 2012. Seasonal and interannual coupling between sea surface temperature, phytoplankton and meroplankton in the subtropical south-western Atlantic Ocean. J. Plankton Res. 34 (3), 236–244. https://doi.org/10.1093/plankt/fbr106.

Godø, O.R., Samuelsen, A., Macaulay, G.J., Patel, R., Hjøllo, S.S., Horne, J., Kaartvedt, S., Johannessen, J.A., 2012. Mesoscale eddies are oases for higher trophic marine life. PLoS One 7 (1), e30161.

Hidaka, K., Kawaguchi, K., Murakami, M., Takahashi, M., 2001. Downward transport of organic carbon by diel migratory micronekton in the western equatorial Pacific: its quantitative and qualitative importance. Deep-Sea Res. I. 48, 1923–1939, 2001.

Hunt Jr., G.L., Stabeno, P.J., Walters, G.E., Sinclair, E.H., Brodeur, R.D., Napp, J.M., Bond, N.A., 2002. Climate change and control of the southeastern Bering Sea pelagic ecosystem. Deep-Sea Res. II, Topical Studies Oceanograph. 49 (26), 5821–5853.

Irigoien, X., Klevjer, T.A., Røstad, A., Martinez, U., Boyra, G., Acuña, J.L., Bode, A., Echevarria, F., Gonzalez-Gordillo, J.I., Hernandez-Leon, S., Agusti, S., Aksnes, D.L., Duarte, C.M., Kaartvedt, S., 2014. Large mesopelagic fishes biomass and trophic efficiency in the open ocean. Nat. Commun. 5, 3271.

Johnson, G.C., Stabeno, P.J., Riser, S.C., 2004. The Bering slope current system revisited. J. Phys. Oceanogr. 34 (2), 384–398.

Johnson, D.S., Sinclair, E.H., 2017. Modeling joint abundance of multiple species using Dirichlet process mixtures. Environmetrics 28 (3), e2440.

Jónasdóttir, S.H., Visser, A.W., Richardson, K., Heath, M.R., 2015. Seasonal copepod lipid pump promotes carbon sequestration in the deep. North Atlantic PNAS 112 (39), 12122–12126.

Kinder, T.H., Coachman, L.K., Galt, J.A., 1975. The Bering slope current system. J. Phys. Oceanogr. 5 (2), 231–244.

Kinder, T.H., Hunt Jr., G.L., Schneider, D., Schumacher, J.D., 1983. Correlations between seabirds and oceanic fronts around the Pribilof Islands, Alaska. Estuarine. Coastal Shelf Sci. 16, 309–331. https://doi.org/10.1016/0272-7714(83)90148-8.

Ladd, C., 2014. Seasonal and interannual variability of the bering slope current. Deep Sea Res. Part II Top. Stud. Oceanogr. 109, 5–13.

Ladd, C., Stabeno, P.J., O'Hern, J.E., 2012. Observations of a Pribilof eddy. Deep Sea Res. Oceanogr. Res. Pap. 66, 67–76.

Longhurst, A.R., Harrison, W.G., 1988. Vertical nitrogen flux from the oceanic photic zone by diel migrant zooplankton and nekton. Deep-Sea Res. 35, 881–889.

Loughlin, T.R., Sukhanova, I.N., Sinclair, E.H., Ferrero, R.C., 1999. Summary of biology and ecosystem dynamics in the Bering Sea. In: Loughlin, T.R., Ohtani, K. (Eds.), Dynamics of the Bering Sea. University of Alaska Sea Grant, Fairbanks.

MacQueen, J.B., 1967. Some methods for classification and analysis of multivariate observations. In: Le Cam, L.M., Neyman, J. (Eds.), Proceedings of the Fifth Berkeley Symposium on Mathematical Statistics and Probability, vol. 1. University of California Press, California, pp. 281–297.

Mecklenburg, C.W., Mecklenburg, T.A., Thorsteinson, L.K., 2002. Fishes Of Alaska. American Fisheries Society, Bethesda, Maryland et al. 2002.

McGillicuddy Jr., D.J., 2016. Mechanisms of physical-biological-biogeochemical interaction at the oceanic mesoscale. Ann. Rev. Mar. Sci 8, 125–159. https://doi.org/10.1146/annurev-marine-010814-015606.

Mizobata, K., Saitoh, S.I., 2004. Variability of Bering Sea eddies and primary productivity along the shelf edge during 1998–2000 using satellite multisensor remote sensing. J. Mar. Syst. 50 (1–2), 101–111.

Mizobata, K., Wang, J., Saitoh, S., 2006. Eddy-induced cross-slope exchange maintaining summer high productivity of the Bering Sea shelf break. J. Geophys. Res. Atmos. 111 (C10) https://doi.org/10.1029/2005JC003335.

NASA Goddard Space Flight Center, 2018. Ocean Ecology Laboratory, Ocean Biology Processing Group (OBPG), 2018: Sea-Viewing Wide Field-Of-View Sensor (SeaWiFS) Chlorophyll Data. Reprocessing. NASA OB.DAAC, Greenbelt, MD, USA. https://doi.org/10.5067/ORBVIEW-2/SEAWIFS/L3M/CHL/2018. (Accessed 11 December 2018).

NOAA, National Marine Fisheries Service, 2007. Conservation plan for the eastern pacific stock of northern Fur seal, Callorhinus ursinus. Available: https://www.fisheries.noaa.gov/species/northern-fur-seal, 137.

Nordstrom, C.A., Battaile, B.C., Cotte, C., Trites, A.W., 2013. Foraging habitats of lactating northern Fur seals are structured by thermocline depths and submesoscale fronts in the eastern Bering Sea. Deep Sea Res. Part II Top. Stud. Oceanogr. 88, 78–96.

Panteleev, G., Yaremchuk, M., Luchin, V., Nechaev, D., Kukuchi, T., 2012. Variability of the Bering Sea circulation in the period 1992–2010. J. Oceanogr. 68, 485–496. https://doi.org/10.1007/s10872-012-0113-0.

Panteleev, G., Luchin, V., Nezlin, N.P., Kikuchi, T., 2013. Seasonal climatologies of oxygen and phosphates in the Bering Sea reconstructed by variational data assimilation approach. Polar Sci. 7 (3–4), 214–232. https://doi.org/10.1016/j.polar.2013.10.001.

Paredes, R., Harding, A.M.A., Irons, D.B., Roby, D.D., Suryan, R.M., Orben, R.A., Renner, H., Young, R., Kitaysky, A., 2012. Proximity to multiple foraging habitats enhances seabirds' resilience to local food shortages. Mar. Ecol.: Prog. Ser. 471, 253–269.

Paredes, R., Orben, R.A., Suryan, R.M., Irons, D.B., Roby, D.D., Harding, A.M.A., Young, R.C., Benoit-Bird, K., Ladd, C., Renner, H., Heppell, S., Phillips, R.A., Kitaysky, A., 2014. Foraging responses of black-legged kittiwakes to prolonged food-shortages around colonies on the Bering Sea shelf. PLoS One 9 (3), e92520. https://doi.org/10.1371/journal.pone.0092520.

Parekh, P., Dutkiewicz, S., Follows, M.J., Ito, T., 2006. Atmospheric carbon dioxide in a less dusty world. Geophys. Res. Lett. 33, L03610. https://doi.org/10.1029/2005GL025098.

Pearcy, W.G., Nemoto, T., Okiyama, M., 1979. Mesopelagic fishes of the Bering Sea and adjacent northern North Pacific Ocean. J. Oceanogr. Soc. Jpn. 35 (3–4), 127–135.

Prants, S.V., Andreev, A.G., Uleysky, M. Yu, Budyansky, M.V., 2019. Lagrangian study of mesoscale circulation in the Alaskan Stream area and the eastern Bering Sea. Deep sea research II. Topical Studies Oceanograph. 169–170. https://doi.org/10.1016/j.dsr2.2019.03.005.

Proud, R., Cox, M.J., Brierley, A.S., 2017. Biogeography of the global ocean's mesopelagic zone. Curr. Biol. 27 (1), 113–119. https://doi.org/10.1016/j.cub.2016.11.003.

R Core Team, 2019. R: A Language and Environment for Statistical Computing. R Foundation for Statistical Computing, Vienna, Austria. https://www.R-project.org/.

Radchenko, V.I., 2007. Mesopelagic fish community supplies "biological pump". In: The Raffles Bulletin Zoological Supplement, 14, pp. 265–271.

Reed, R.K., Stabeno, P.J., 1994. Flow along and across the aleutian ridge. J. Mar. Res. 52, 639–648.

Reed, R.K., Stabeno, P.J., 1999. The Aleutian North slope current. In: Loughlin, T.R., Ohtani, K. (Eds.), Dynamics of the Bering Sea: A Summary of Physical, Chemical, and Biological Characteristics, and a Synopsis of Research on the Bering Sea. University of Alaska Sea Grant, pp. 177–191. AK-SG-99-03, North Pacific Marine Science Organization (PICES).

Reynolds, R.W., Smith, T.M., Liu, C., Chelton, D.B., Casey, K.S., Schlax, M.G., 2007. Daily high-resolution-blended analyses for sea surface temperature. J. Clim. 20, 5473–5496.

Roden, G.I., 1995. Aleutian Basin of the Bering Sea: thermohaline, oxygen, nutrient, and current structure in july 1993. J. Geophys. Res.: Oceans 100 (C7), 13539–13554.

Saijo, D., Mitani, Y., Abe, T., Sasaki, H., Goetsch, C., Costa, D.P., Miyashita, K., 2017. Linking mesopelagic prey abundance and distribution to the foraging behavior of a deep-diving predator, the northern elephant seal. Deep Sea Res. Part II Top. Stud. Oceanogr. 140, 163–170.

St John, M.A., Borja, A., Chust, G., Heath, M., Grigorov, I., Mariani, P., Martin, A.P., Santos, R.S., 2016. A dark hole in our understanding of marine ecosystems and their services: perspectives from the mesopelagic community. Front. Mar. Sci. 6. https://doi.org/10.3389/fmars.2016.00031.

Schneider, D.C., Harrison, N.M., Hunt Jr., G.L., 1990. Seabird diet at a front near the Pribilof Islands, Alaska. Stud. Avian Biol. 14, 61–66.

Shono, H., 2008. Application of the Tweedie distribution to zero-catch data in CPUE analysis. Fish. Res. 93 (1–2), 154–162.

Sinclair, E.H., 1991. Review of the biology and distribution of the neon flying squid (*Ommastrephes bartrami*) in the north Pacific Ocean. In: U.S. Dep. Commer. NOAA Tech. Rept. NMFS 105, pp. 57–67.

Sinclair, E.H., Stabeno, P.J., 2002. Mesopelagic nekton and associated physics of the southeastern Bering Sea. Deep-Sea Res. II 49, 6127–6145.

Sinclair, E., Loughlin, T., Pearcy, W., 1994. Prey selection by northern Fur seals (*Callorhinus ursinus*) in the eastern Bering Sea. Fish. Bull. 92, 144–156.

Sinclair, E.H., Balanov, A.A., Kubodera, T., Radchenko, V.I., Fedorets, Y.A., 1999. Distribution and ecology of mesopelagic fishes and cephalopods. In: Loughlin, T.R., Ohtani, K. (Eds.), Dynamics of the Bering Sea. University of Alaska Sea Grant, Fairbanks, pp. 485–508.

Sinclair, E.H., Vlietstra, L.S., Johnson, D.S., Zeppelin, T.K., Byrd, G.V., Springer, A.M., Ream, R.R., Hunt Jr., G.L., 2008. Patterns in prey use among Fur seals and seabirds in the Pribilof Islands. Deep-Sea Res. II 55, 1897–1918.

Sinclair, E.H., Walker, W.A., Thomason, J.R., 2015. Body size regression formulae, proximate composition and energy density of eastern Bering Sea mesopelagic fish and squid. PLoS One 10 (8), e0132289. https://doi.org/10.1371/journal.pone.0132289.

Sinclair, E.H., Walker, W.A., Thomason, J.R., 2016. Correction: body size regression formulae, proximate composition and energy density of eastern Bering Sea mesopelagic fish and squid. PLoS One 11 (7), e0159353. https://doi.org/10.1371/journal.pone.0159353. Open Access.

Springer, A.M., McRoy, C.P., Flint, M.V., 1996. The Bering Sea green belt: shelf-edge processes and ecosystem production. Fish. Oceanogr. 5 (3-4), 205–223.

Stabeno, P.J., Van Meurs, P., 1999. Evidence of episodic on-shelf flow in the southeastern Bering Sea. J. Geophys. Res. https://doi.org/10.1029/1999JC900242.

Stabeno, P.J., Ladd, C., Reed, R.K., 2009. Observations of the Aleutian North slope current, Bering Sea, 1996–2001. J. Geophys. Res. 114, C05015. https://doi.org/10.1029/2007JC004705.

Stabeno, P.J., Danielson, S., Kachel, D., Kachel, N.B., Mordy, C.W., 2016. Currents and transport on the eastern Bering Sea shelf: an integration of over 20 years of data. Deep Sea Res. Part II 134, 13–29. https://doi.org/10.1016/j.dsr2.2016.05.010, 2016.

Stabeno, P.J., Hristova, H.G., 2014. Observations of the alaskan Stream near Samalga pass and its connection to the Bering Sea: 2001–2004. Deep Sea Res. Oceanogr. Res. Pap. 88, 30–46. https://doi.org/10.1016/j.dsr.2014.03.002.

Sterling, J.T., 2009. Northern Fur Seal Foraging Behaviors, Food Webs, and Interactions with Oceanographic Features in the Eastern Bering Sea. School of Aquatic and Fishery Sciences, University of Washington, p. 209. PhD. Thesis.

Sutton, T.T., Clark, M.R., Dunn, D.C., Halpin, P.N., Rogers, A.D., Guinotte, J., Bograd, S. J., Angel, M.V., Perez, J.A.A., Wishner, K., Haedrich, R.L., Lindsay, D.J., Drazen, J. C., Vereshchaka, A., Piatkowski, U., Morato, T., Błachowiak-Samołyk, K., Robison, B. H., Gjerde, K.M., Pierrot-Bults, A., Bernal, P., Reygondeau, G., Heino, M., 2017. A global biogeographic classification of the mesopelagic zone. Deep-Sea Res. Part I 126, 85. https://doi.org/10.1016/j.dsr.2017.05.006, 10286.

Vecchione, M., Falkenhaug, T., Sutton, T., Cook, A., Gislason, A., Hansen, H.O., Heino, M., Miller, P.I., Piatkowski, U., Porteiro, F., Soiland, H., Bergstad, O.A., 2015. The effect of the North Atlantic Subpolar Front as a boundary in pelagic biogeography decreases with increasing depth and organism size. Prog. Oceanogr. 138, 105–115. https://doi.org/10.1016/j.pocean.2015.08.006.

Walker, W.A., Jones, L.L., 1991. Food habits of northern right whale dolphin, Pacific white-sided dolphin, and northern Fur seal caught in the high seas driftnet fisheries of the North Pacific Ocean, 1990. In: Ito, J., Shaw, W., Burgner, R.L. (Eds.), International North Pacific Fisheries Commission, Symposium on Biology, Distribution and Stock Assessment of Species Caught in the High Seas Driftnet Fisheries in the North Pacific Ocean, Bulletin, vol. 53, pp. 285–295 (II).

Willis, J.M., Pearcy, W.G., 1982. Vertical distribution and migration of fishes of the lower mesopelagic zone off Oregon. Mar. Biol. 70, 87–98.

Wood, S.N., 2011. Fast stable restricted maximum likelihood and marginal likelihood estimation of semiparametric generalized linear models. J. Roy. Stat. Soc. B 73 (1), 3–36. Wiley Online Library.

Wood, S.N., 2017. Generalized Additive Models: an Introduction with R. Chapman; Hall/CRC.

Wood, S.N., Pya, N., Säfken, B., 2016. Smoothing parameter and model selection for general smooth models. J. Am. Stat. Assoc. 111 (516).